UNIVERSITY OF CALIFORNIA
RIVERSIDE

Aerosol Spray Pyrolysis Synthesis of CZTS Nanostructures for Photovoltaic Applications

A Thesis submitted in partial satisfaction
of the requirements for the degree of

Master of Science

in

Mechanical Engineering

by

Stephen Exarhos

August 2015

Thesis Committee:
Dr. Lorenzo Mangolini, Chairperson
Dr. Marko Princevac
Dr. Sandeep Kumar

The Thesis of Stephen Exarhos is approved:

_____

_____

_____
Committee Chairperson

University of California, Riverside

Acknowledgements

I acknowledge the use of work published previously in the journal **Chemical Communications**, Issue 77 (August, 2014) titled, "Spray Pyrolysis of CZTS Nanoplatelets." I am the primary contributor for this article, while Dr. Krassimir Bozhilov (University of California, Riverside, Department of Materials Science and Engineering, Central Facility for Advanced Microscopy and Microanalysis) and Dr. Lorenzo Mangolini (University of California, Riverside, Department of Mechanical Engineering and Department of Materials Science and Engineering) are also acknowledged as contributors. I would particularly like to acknowledge Dr. Bozhilov for his impressive contribution to TEM characterization of CZTS nanoplatelets shown in Section 4.1.

I also acknowledge financial support provided by Dr. Mangolini via NSF BRIGE award number 1125660 and NSF CAREER award number 1351386.

I would also like to acknowledge meaningful contributions to my work by former undergraduate assistant Jesus Hernandez and PhD student Alejandro Alvarez, both members of Dr. Mangolini's research group.

ABSTRACT OF THE THESIS

Aerosol Spray Pyrolysis Synthesis of CZTS Nanostructures
for Photovoltaic Applications

by

Stephen Exarhos

Master of Science, Graduate Program in Mechanical Engineering
University of California, Riverside, August 2015
Dr. Lorenzo Mangolini, Chairperson

As harmful effects caused by the extraction, purification, and combustion of natural resources for energy generation become more clearly understood, the need for economically competitive renewable energy becomes more desirable. Solar energy-generation is a technologically feasible method, though its primary drawback is cost. Traditional single-crystal silicon-based photovoltaics are too expensive to compete with nonrenewable energy generation, while alternative materials such as cadmium telluride and copper-indium-gallium-selenide contain expensive and unsustainable elements, while cadmium is a known carcinogen. Copper-zinc-tin-sulfide (CZTS) is an another alternative material, though the technology is not yet advanced enough to have reached the market.

The work presented is a study of the viability of synthesizing CZTS nanostructures using aerosol spray pyrolysis in an inexpensive, environmentally friendly, and industry-scalable way. We aerosolize a precursor solution with dissolved copper, zinc, and tin compounds and pass the droplets through a furnace, where the precursors

dissolve and thermally form CZTS structures. Using this method, we can generate thin films — by placing a substrate within the furnace — and nanoparticles. While stoichiometric CZTS seems to be formed consistently, the films grown tend to be inhomogeneous in composition and morphologically unstable, yielding an inefficient material for two-dimensional photovoltaics. Nanoparticle synthesis seems to be the more appropriate application of spray pyrolysis with this material system. We have shown the ability to control the composition and doping of CZTS nanoparticles, and preliminary efforts in coating and sintering the nanoparticles into crystalline films are promising.

Table of Contents

Chapter 1: Introduction/Motivation ……..1
1.1: A Background on Photovoltaics ……..1

1.2: Thesis Direction ……..6

1.3: References ……..8

Chapter 2: Literature Review ……..9
2.1: Notable Terms and Quantities ……..9

2.2: Current CZTS Benchmarks ……10

2.3: Ways to Improve CZTS-Based PV Efficiency ……10

2.4: Material Synthesis ……12

2.5: Spray Pyrolysis Synthesis of CZTS Thin Films ……19

2.6: CZTS Nanoparticle Synthesis ……20

2.7: CZTS Sintering/Annealing ……22

2.8: CZTS Thin Film and Nanoparticle Characterization ……23

2.9: References ……25

Chapter 3: Experimental ……39
3.1: Precursor Synthesis ……39

3.2: Precursor Solution Chemistry ……41

3.3: Synthesizing CZTS Thin Films/Platelets……43

3.4: Synthesizing CZTS Nanoparticles ……45

3.5: Doping CZTS Nanoparticles ……47

3.6: Coating CZTS Dispersions onto Substrates ……47

3.7: Sintering CZTS Nanoparticles to form Crystalline Films ……50

3.8: References ……51

Chapter 4: Results ……52
4.1: Synthesis of CZTS Thin Films/Platelets ……52

4.2: Synthesis of CZTS Nanoparticles ……57

4.3: Doping of CZTS Nanoparticles ……61

4.4: CZTS Nanoparticle Annealing ……64

4.5: References ……67

Chapter 5: Conclusions/Recommendations ……68
5.1: Conclusions ……68

5.2: Future Work ……70

List of Figures

Chapter 1: Introduction/Motivation ……..1
1.1.1 General PV Schematic ……..2

1.1.2 Domestic Energy Trends ……..3

1.1.3 Cost and Abundance of PV-Related Materials ……..4

1.1.4 CIGS and CZTS Crystal Structures ……..5

Chapter 2: Literature Review ……..9
2.4.1 General Evaporation Schematic……13

2.4.2 General Sputtering Schematic ……14

2.4.3 General Electrodeposition Schematic ……15

2.4.4 General Pulsed Laser Deposition Schematic ……17

2.4.5 General Chemical Bath Deposition Schematic ……18

2.5.1 General Thin Film Aerosol Spray Pyrolysis Schematic ……19

Chapter 3: Experimental ……39
3.1.1 Thermogravimetric Analysis of CZTS Precursors ……39

3.2.1 Quasi-Ternary CZTS Phase Diagram ……41

3.2.2 EDS of Compositionally Varied CZTS ……42

3.3.1 Thin Film Aerosol Spray Pyrolysis Schematic ……43

3.4.1 Nanoparticle Aerosol Spray Pyrolysis Schematic ……45

3.6.1 Example CZTS Nanoparticle Coating ……48

3.7.1 Sulfur-Annealing Ampoule ……49

Chapter 4: Results ……52
4.1.1 Thin Film SEM Images ……52
4.1.2 Binary Sulfide Thin Film SEM Images ……53
4.1.3 XRD and UV-vis Absorbance of CZTS Thin Film ……53
4.1.4 Raman of CZTS Thin Films ……54
4.1.5 TEM Analysis of CZTS Platelet ……55
4.2.1 CZTS Nanoparticle TEM Image and Diffraction ……57
4.2.2 XRD and Raman of CZTS Nanoparticle ……57
4.2.3 Raman of CZTS Nanopowders ……59
4.2.4 TEM of High-Temperature CZTS Nanoparticle ……59
4.3.1 EDS Showing Sodium Doping Amounts ……61
4.3.2 XRD of Si-Doped CZTS ……63
4.4.1 SEM of Annealed CZTS Coatings ……64
4.4.2 EDS Maps of Annealed CZTS Coating ……65

List of Equations

Chapter 2: Literature Review ……..9
2.1.1 Fill Factor Definition ……..9

2.1.2 Photo-Conversion Efficiency Definition ……..9

List of Tables

Chapter 4: Results ……52
4.1.1 EDS of CZTS Thin Films ……55

4.1.2 EDS of CZTS Nanoparticles ……60

Chapter 1: Introduction/Motivation

1.1: A Background on Photovoltaics

The ability to harness the sun's energy incident on Earth's surface has long been touted as a large-scale electricity source of the future. The drawback thus far, though, has been cost-effectiveness. As limitations and harmful effects on burning nonrenewable resources as fuel have become more and more well documented in the past half-century, photovoltaic (PV) research has garnered significant interest in the international community, among other renewable technologies. The technology currently exists to harness solar energy, but it is not economically or politically tenable to implement large-scale solar power infrastructure. Hence, much work is currently focused on decreasing the cost of PV module fabrication, installation, and maintenance. On the cell fabrication side, a large focus is placed on optimizing alternative and inexpensive light-absorbing materials that can be produced via inexpensive and scalable processes.

French physicist Edward Becquerel is credited with the discovery of the PV effect in the mid-19th century, which, in layman's terms, is observed when a material absorbs a photon with a certain energy to create a pair of excitons, or positively (holes) and negatively (electrons) oriented charge carriers. It took nearly a century for Becquerel's PV effect to be applied as an effective PV cell due to the difficulty of collecting the excitons generated by photo-absorption.

Bell Labs made the major breakthrough in 1954, when Chapin, Fuller, and Pearson demonstrated the first practical solar cell, based on single-crystal silicon as the

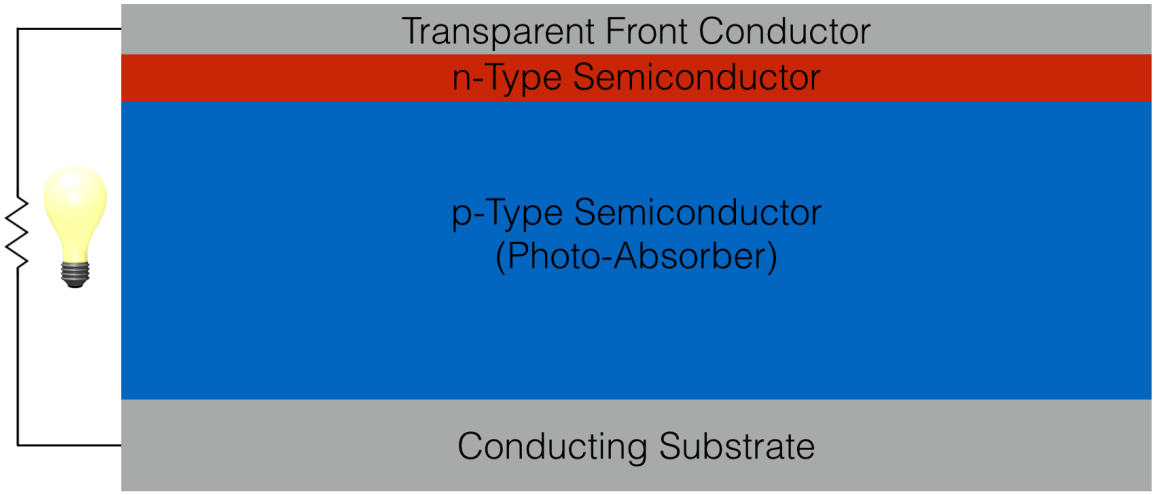

Figure 1.1.1: General schematic for a p-n junction PV similar to that made by Chapin in [1]. (Note: Chapin used a thick n-doped Si layer as the photo-absorber and a thin p-doped Si layer to complete the p-n junction; modern PVs use the layout above.)

photo-absorber [1]. This cell demonstrated a photo-conversion efficiency of 6%. A similar iteration of this cell was fabricated and sold at $1,785 per Watt of power generated by Western Electric in 1955.

Chapin observed that a p-n semiconductor junction will create an electric field to force the exciton pair in opposite directions [1]. This counteracts radiative exciton recombination, the statistically more probable event, making it possible to collect the opposite charges to create a potential difference across a resistive load. The simplified schematic of the p-n junction-driven PV is seen in Fig. 1.1.1. Chapin's work on silicon-based p-n junction PVs has been steadily optimized since 1954, and today the latest iterations of this type of PV are nearing maximum theoretical efficiency.

Alternative material systems have also been studied and gradually optimized to account for the high material and processing costs associated with generating the single-

crystal silicon layer in the cell schematic in Fig. 1.1.1. Yet the cost-per-Watt of power generated still makes solar energy impractical as part of a large-scale infrastructure.

Today, the effort to improve PV technology continues, with the notion of "grid parity" limiting the wide-spread use of PVs in the United States [2]. In essence, the consensus is that PVs will not be wide-spread until it is less expensive to fabricate, implement, and maintain such devices than to purchase mass-produced power generated from nonrenewable sources — like natural gas, coal, oil, or others.

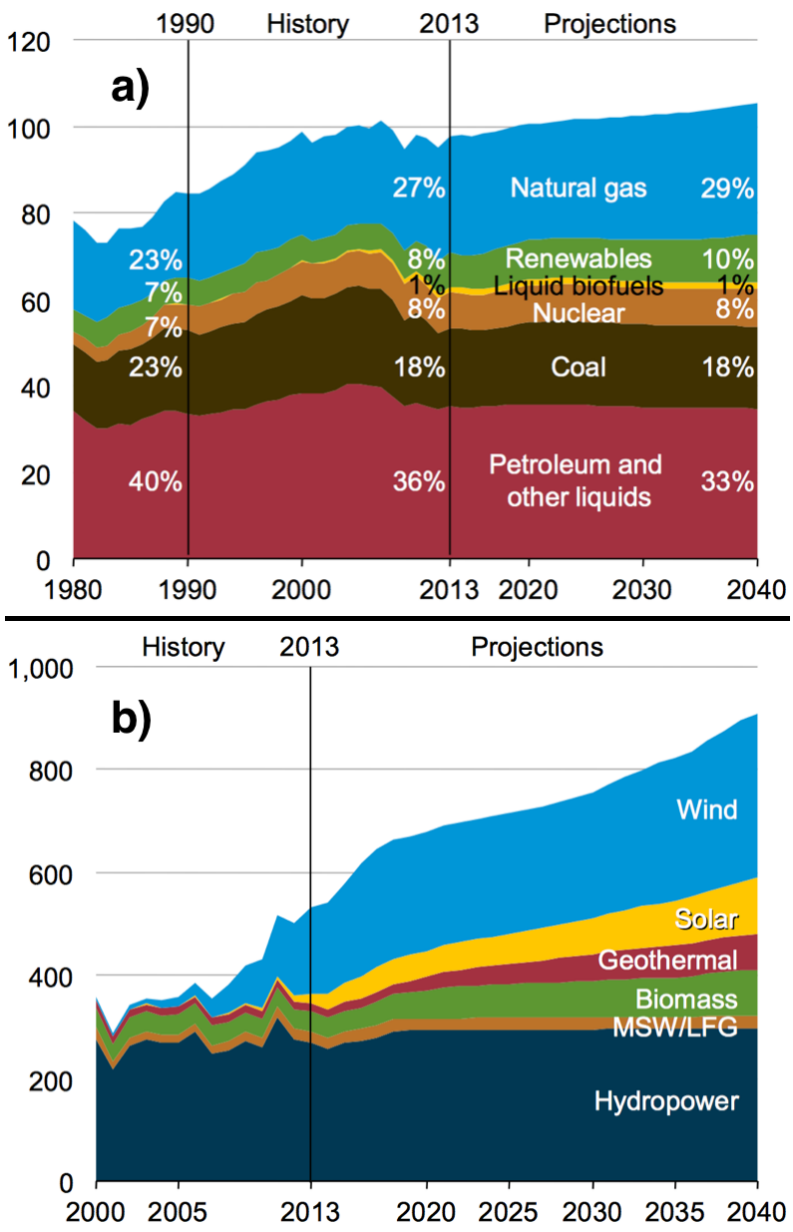

Figure 1.1.2: (From [3]) a) Shows past and projected percentages of energy consumption by fuel type from 1980-2040 in quadrillion BTU. b) Shows past and projected renewable electricity generation by fuel type from 2000-2040 in billion kilowatt hours.

Based on recent trends and public policy, the Department of Energy's annual energy outlook for the year 2015 [3] projects that domestic energy generated by renewable fuels will continue to expand to take the place of domestic nonrenewable-based fuels like petroleum and coal (fig. 1.1.2a). Energy generation from renewable sources is projected to grow at 1.5% annually, more than any other fuel source [3]. Further, domestic solar electricity generation is projected to grow more quickly than any other renewable source at 5.5% annually, and is expected to provide about 10% of all domestic electricity generated by renewable sources in 2040 [3] (fig. 1.1.2b).

In the past few decades, there has been an ongoing search within the PV-research field for new materials and cell architectures that might circumvent the drawbacks to using silicon-based cells — namely that the most efficient single-crystal silicon-based PVs require high production and high materials cost. Thin film PVs — cells based on thin film semiconductors as opposed to bulk, necessary with single-crystal silicon cells — have been well studied utilizing different photo-absorbing materials.

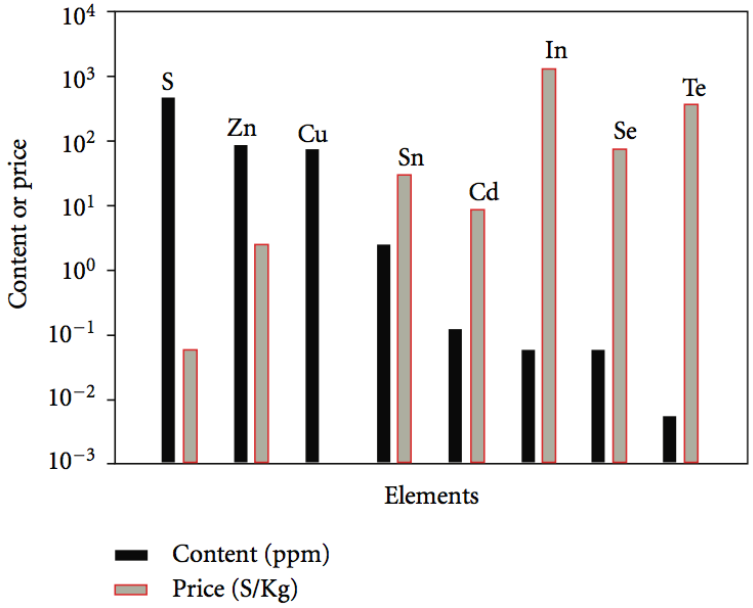

Figure 1.1.3: (From [6]) Shows content and price of elements commonly used in different thin film PV absorber layers.

Copper-indium-gallium-selenide (CIGS) and cadmium telluride (CdTe) have both been extensively researched, and have been improved to be efficient enough to sell publicly via startup companies like First Solar (CdTe) [4] or Solar Frontier (CIGS) [5]. These materials, however, have significant drawbacks pertaining to mass market sustainability and environmental impact. Indium, in particular, is undesirable to use in a mass market product due to its scarcity on earth and its subsequent high cost (fig. 1.1.3), making this technology unsustainable for a large market [6]. Cadmium is a known human carcinogen, making its widespread commercial use undesirable due to possible negative health and environmental effects.

Relatively recently, in the past 25 years, copper-zinc-tin-sulfide — Cu_2ZnSnS_4 (CZTS) — has been investigated as a thin film photo-absorber for use in PV devices. This material is

Figure 1.1.4: (From [8]) Shows chalcopyrite CIGS crystal structure (a) with different CZTS crystal structures (b, c, d).

desirable due to the component elements' low-cost and Earth-abundance (fig. 1.1.3).

CZTS typically has a kesterite crystal structure which resembles the chalcopyrite structure of CIGS, though it can also be found as stannite (which only differs from kesterite in placement of copper and zinc atoms) or as wurtzite. Chen *et al* calculate the kesterite structure to be the most thermodynamically stable of the three crystal structures [7]. Fig. 1.1.4 shows the orientations of the three CZTS crystal structures with the chalcopyrite CIGS crystal structure. The band gap of CZTS is between 1-1.5 eV, and the material has an absorption coefficient on the order of 10^4, both desirable characteristics for use as a photo-absorber in a PV [8]. The primary advantage of using CZTS is that it offsets the drawbacks of silicon, CIGS, and CdTe technologies. Copper, zinc, tin, and sulfur are all relatively inexpensive, earth abundant, and environmentally friendly.

1.2: Thesis Direction

Presented here is our work investigating the viability of forming CZTS nanostructures and thin films by aerosol spray pyrolysis — an inexpensive and scalable technique — from metal-diethyldithiocarbamate precursors. The effect of this work is intended to prove this to be an alternative method of synthesizing high-quality CZTS thin films for use in highly efficient PV cells, while also being easily implemented into commercial-scale production.

There is herein much discussion of the application of CZTS as a photo-absorber layer in PVs, mainly in Chapter 2, though our work itself is to this point only developed as far as free-standing material synthesis and characterization.

1.3: References

[1] D. M. Chapin, C. S. Fuller. “A New Silicon P−n Junction Photocell for Converting Solar Radiation into Electrical Power.” Journal of Applied Physics 25, no. 5 (1954): 676–77. doi:10.1063/1.1721711.

[2] Breyer, Christian, and Alexander Gerlach. “Global Overview on Grid-Parity.” Progress in Photovoltaics: Research and Applications 21, no. 1 (January 1, 2013): 121–36. doi:10.1002/pip.1254.

[3] Holtberg, Paul, Skelly, Dan, Kondis, Paul, *et al*. “Annual Energy Outlook 2015 with projections to 2040.” U.S. Energy Information Administration. (April, 2015). <www.eia.gov/forecasts/aeo>.

[4] “First Solar Sets World Record for CdTe Solar PV Efficiency.” First Solar, Inc. News provided by Acquire Media (July 26, 2011). <http://investor.firstsolar.com/releasedetail.cfm?ReleaseID=593994>.

[5] “Company Overview of Solar Frontier K.K.” Business Week (July 2, 2015). <http://www.bloomberg.com/research/stocks/private/snapshot.asp?privcapId=52311569>.

[6] Wang, Hongxia. “Progress in Thin Film Solar Cells Based on CZTS.” International Journal of Photoenergy 2011 (September 4, 2011): e801292. doi:10.1155/2011/801292.

[7] Chen, Shiyou, X. G. Gong, Aron Walsh, and Su-Huai Wei. “Crystal and Electronic Band Structure of Cu2ZnSnX4 (X=S and Se) Photovoltaic Absorbers: First-Principles Insights.” Applied Physics Letters 94, no. 4 (January 26, 2009): 041903. doi:10.1063/1.3074499.

[8] Jiang, Minlin, and Xingzhong Y. “Cu2ZnSnS4 Thin Film Solar Cells: Present Status and Future Prospects.” In Solar Cells - Research and Application Perspectives, edited by Arturo Morales-Acevedo. InTech, 2013. <http://www.intechopen.com/books/solar-cells-research-and-application-perspectives/cu2znsns4-thin-film-solar-cells-present-status-and-future-prospects>.

Chapter 2: Literature Review

2.1: Notable Terms and Quantities

There are several terms and quantities that are used to describe the efficacy of PVs, the most notable of which are open circuit voltage (V_{OC}), short circuit current (J_{SC}), fill factor (FF), and photo-conversion efficiency (η). V_{OC} is defined as the potential difference generated by a PV across an effectively infinite load between the positive and negative charge collection terminals. J_{SC} is is the electrical current flowing through the circuit when the load is effectively zero. There is an absolute extreme at which the PV will supply the most power, given by P_m or equivalently I_m*V_m. This allows the definition of FF as

$$FF = \frac{I_m \times V_m}{I_{SC} \times V_{OC}} \qquad \text{Eq. 2.1.1}$$

and η as

$$\eta = \frac{P_m}{P_L} \qquad \text{Eq. 2.1.2}$$

where P_L is the power of the light incident on the PV. P_L is generally simulated *in vitro* [1].

For discussion in literature, it is globally accepted that PVs be characterized under the Standard Test Conditions: 25 ºC under Air Mass 1.5 spectrum illumination with an incident power density of 100 mW/cm^2 [1].

2.2: Current CZTS Benchmarks

The current champion CZTS cell is presented by Fukano *et al* in [3]. The record efficiency was published to be 8.5% ± 0.2% for a cell of 0.2382 cm^2. The V_{OC} is listed as 708 mV and the J_{SC} is listed as 16.83 mA/cm^2, while the FF is 70.9% [2, 3]. To give perspective, the current champion CIGS cell has η listed as 21.7% ± 0.7%. The V_{OC} is comparable, as the CIGS cell has V_{OC} as 796.3 mV, but the J_{SC} of the CIGS cell is vastly superior at 36.59 mA/cm^2 and the FF is improved to 79.3% [2, 4].

There has been extensive work done optimizing CZTS PVs by introducing selenium replacement defects in place of sulfur atoms in the kesterite lattice, with the new material called CZTSSe ($Cu_2ZnSn(S_xSe_{1-x})_4$). With this material system, a cell has been produced by Wang *et al* with η listed as 12.6% ± 0.3%, with improved J_{SC} of 35.21 mA/cm^2 but diminished V_{OC} of 513.4 mV [2, 5]. While this is an encouraging improvement in photo-conversion efficiency, the material system will be disregarded in this work due to the inclusion of the rare and expensive element, selenium (see fig. 1.1.3).

In order for CZTS to be commercialized viably, it is generally accepted that the *in vitro* photo-conversion efficiency needs to be boosted to ~17-18%.

2.3: Ways to Improve CZTS-Based PV Efficiency

Due to the similarities between the CIGS and the CZTS material systems, it is logical to attempt to improve CZTS-based PVs in similar manners as have already proven effective in the improvement of CIGS-based PVs to beyond 20% efficient.

In 2013, a meeting of experts in the field was convened to identify critical steps toward improving CZTS as a thin film PV material [6]. The V_{OC} deficit (given by the difference between the the band gap voltage — E_g/q — and the V_{OC}) in well-performing CIGS-based PVs is ~500 mV, while in the best CZTSSe devices the deficit is higher than 650 mV. From section 2.2, the benchmark CZTS device in [3] has a V_{OC} of 708 mV, which still yields a V_{OC} deficit of greater than 750 mV.

Quoting from [6]:

> *"Three key areas were identified to address this problem, as listed here in rough order of priority: (1) defect characterization and passivation, (2) phase stability and processing control, and (3) interface optimization."*

Further from [6], defects in the CZTS layer cause the semiconducting properties of the material — primarily the band gap — to be nonuniform through the bulk material, leading to additional impedance affecting the generated excitons. The high V_{OC} loss is attributed to charge recombination centers, focused at bulk defect sites as well as grain boundaries and interfaces. The formation and control of these defects is not well understood at this point. With further understanding will come the ability to promote beneficial defects and to diminish detrimental ones in the synthesis of the CZTS absorber layer. The pn-junction also must be optimized in order to reduce interfacial exciton recombination.

Current work on improving the CZTS absorber layer focuses generally on improving the material stoichiometry [7-12] and crystallinity [13-17] within existing

synthesis processes. Further efforts are focused on improving the pn-junction consisting of the CZTS and a thin n-type layer [18-20]. In short, it has been concluded that the ideal stoichiometry is slightly copper-poor and zinc-rich, that the presence of alkali metal defects in CZTS greatly aid crystal growth during annealing, and that ZnS is likely the ideal n-type material to pair with CZTS. Further work must be done to support these conclusions more solidly, though this is generally consensus in the field as observed at the 2015 MRS Spring Meeting.

2.4: Material Synthesis

There are many different methods that have been used to generate CZTS or CZTSSe. The previously-mentioned CZTSSe benchmark was set in 2013 for a cell based on a CZTSSe layer grown using a hydrazine pure-solution approach [5]. The benchmark CZTS cell was made by sputtering ZnS/Sn/Cu/ZnS layers then annealing in a sulfur-rich atmosphere [3]. Further methods that have been used to synthesize CZTS layers for PVs are evaporation [21-32], sputtering [33-45], electrodeposition [46-53], sol-gel based deposition [54-62], pulsed laser deposition [63-68], screen printing [69-70], chemical bath deposition [71-75], nanoparticle based sintering [76-89], and aerosol spray pyrolysis [90-98].

Of these synthesis methods, evaporation, sputtering, and electrodeposition have generally yielded the highest efficiency devices. Other methods are primarily intended as more cost-effective or scalable alternatives.

Aerosol spray pyrolysis will be discussed further in section 2.5. Nanoparticle synthesis and sintering will be discussed further in sections 2.6 and 2.7.

Evaporation:

Evaporation is a commonly used process to synthesize metallic or semiconducting thin films. The target material, in liquid or more typically solid phase, is evaporated by a concentrated electron beam, directed by Coulombic force, and directed onto a substrate [99] (fig. 2.4.1). Typically, evaporation of the target will be incited by an electron beam, but it can also be achieved thermally. This process can be done with an individual target, or multiple targets can be used simultaneously. For example, a cuprous sulfide thin film can be formed by co-evaporating copper and sulfur targets.

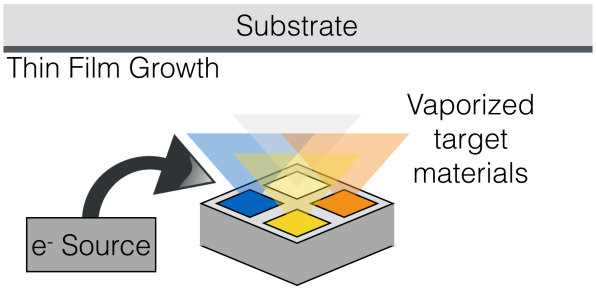

Figure 2.4.1: General schematic for a multi-target electron beam evaporator.

There are two common methods by which evaporation is used to synthesize CZTS. Katagiri *et al* pioneered the method by evaporating separate copper, zinc, and tin layers onto a heated molybdenum-coated soda lime glass substrate, then thermally annealing in an N_2 + H_2S environment [21, 22]. The material was characterized to be stannite CZTS. The stoichiometry of the material was governed by the relative thickness of the three metallic layers.

Other groups have added sulfur in the evaporation process, either via the replacement of the zinc target with a zinc sulfide target [23-26, 31], or the addition of a sulfur target to the three elemental targets [27].

Some of the most efficient CZTS-based PVs to have been reported have all been fabricated with a co-evaporated CZTS layer with an added thermal annealing process.

Sputtering:

Sputtering is also a commonly known process. It is similar to e-beam evaporation, but the target material is eroded away by a gaseous ion plasma, typically made from an inert carrier gas like argon, instead of an electron beam. Neutral particles of the target material ejected from the target then nucleate and form a thin film on the substrate surface [100] (fig. 2.4.2). Similar to evaporation, this process can use multiple targets to form alloy thin films.

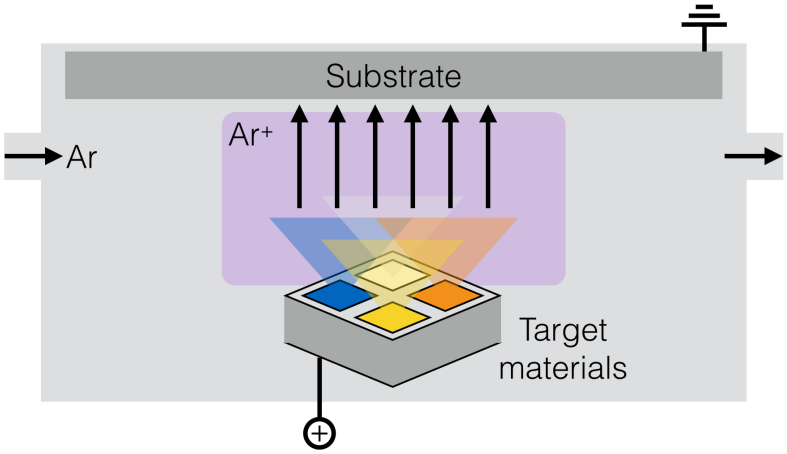

Figure 2.4.2: General schematic for a multi-target sputterer.

Sputtered synthesis of polycrystalline stannite CZTS was first reported by Ito and Nakazawa in 1988 [33]. They reported an improved quality film with decreasing resistivity as substrate temperature during film growth was increased. The conclusion drawn was that CZTS is a suitable absorber layer for a PV due to its high absorption coefficient and its direct band gap.

Again similar to evaporation, there has been work reported as having synthesized CZTS via thermal annealing of a sputtered stack of copper, zinc, and tin metals [35, 36, 40, 41, 44], as well as work reporting the sputtering of binary sulfide targets — most commonly in the form of tin sulfide and zinc sulfide with elemental copper [37-39, 42, 43, 45].

Sputtering deposition creates films of a similar quality to evaporation, so it is not surprising that sputtering-deposited CZTS-based PVs have similarly impressive efficiencies to those synthesized via evaporation, including the current benchmark in [3].

Electrodeposition:

Electrodeposition uses precursor materials dissolved in an electrolyte to complete a circuit across two electrodes, with the current flowing between the electrodes through the electrolyte causing the dissociation of the precursors and deposition onto the working electrode [101] (fig. 2.4.3). Electrodeposition is more dependent on precursor materials than processing conditions, as opposed to the previously discussed vapor deposition processes. The process is presented as more inexpensive and scalable than vacuum-based vapor deposition processes.

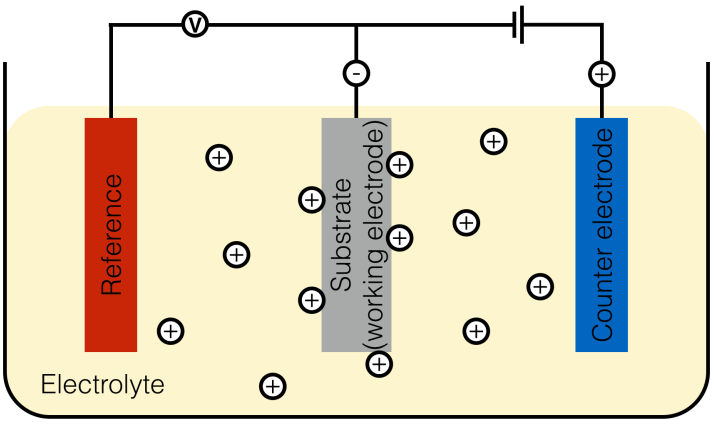

Figure 2.4.3: General schematic for an electrodeposition setup.

To make CZTS, there are a variety of precursors that can be used. Scragg *et al* demonstrated the synthesis of a copper-tin-zinc metal stack via electrodeposition, followed by a sulfur-vapour annealing step to make CZTS. The work used three separate deposition steps, the each using a singular copper, tin, or zinc chloride as the precursor dissolved in the electrolyte [47]. There has been further work via the same precursor chemistry in [46, 49, 51]. There has also been some study of single-step electrodeposition of CZTS by combining copper, zinc, and tin sulfates with sodium thiosulfate in the electrolytic solution in [53], as well as further single-step depositions in [47, 48, 50, 52].

Ahmed *et al* reported a 7.3% efficient CZTS-based PV in [46], the highest value yet reported for this sort of process, based on a thermally annealed electrodeposited three-metal stack of copper, zinc, and tin.

Sol-Gel Deposition:

The sol-gel deposition is fairly straightforward in concept. Precursor metal salts are dissolved in a mixture of solvent and binder, then coated onto a substrate. Thermal treatment of the coating allows for evaporation of the solvent and decomposition of the precursors. A further annealing step allows for the full conversion to a CZTS thin film [56]. This process is advantageous due to its cost-effectiveness and ability to be run at atmospheric pressure.

The biggest source of variety for CZTS synthesis from the sol-gel deposition method is the use of different precursors and solvents. The highest efficiency cell based on a CZTS layer fabricated in this fashion is outlined in [56]. Su *et al* used a non-aqueous

thiourea-metal-oxygen molecule as the precursor solute, which underwent thermal decomposition at a relatively low temperature to leave a more favorable material behind. Their best cell achieved an efficiency of 5.1%. More commonly used as precursor solutes are copper, zinc, and tin acetates or chlorides with or without a sulfur source added as precursor via thiourea [54, 55, 57-59, 62] ([59] used tin sulfide as the tin source).

Pulsed Laser Deposition:

Pulsed laser deposition (PLD) is a vacuum process similar to evaporation and sputtering. Energy is supplied to a target, typically in the form of a pellet, via a high-energy laser pulse. Material is ablated from the target in the form of ionic plasma, which then settles on a substrate within the chamber [102] (fig. 2.4.4). Targets can be elementary or alloy, allowing for deposition of either simple or complex thin films. These films still require a further annealing step after deposition.

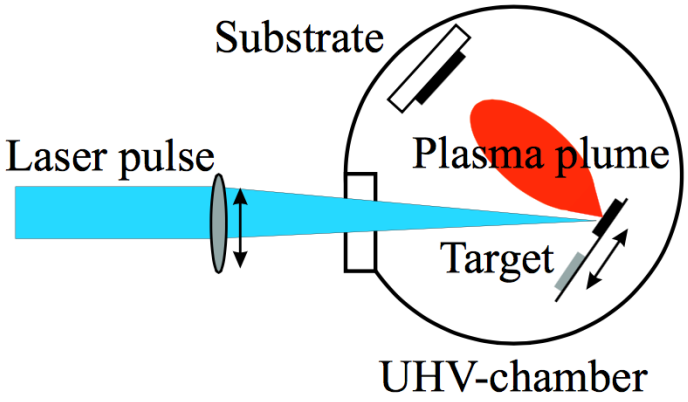

Figure 2.4.4: (From [102]) General schematic for a PLD setup.

The best device fabricated using this method has an efficiency of 3.14% [64]. The PLD deposition was achieved by ablating a target formed by mixing copper, tin, and zinc binary sulfides in adequate ratios into a solid CZTS pellet. Further work studying the PLD deposition of CZTS from a CZTS pellet has been shown in [66, 67]. Moriya pioneered this method of CZTS deposition by depositing a mixture of copper, zinc, and

tin, then annealing in a sulfur atmosphere [63, 65]. Further work has been done using zinc sulfide and copper-tin-sulfide multicomponent targets [68].

Screen Printing:

Screen printing deposition is very similar to sol-gel deposition. It is a solution-phase process by which CZTS particles are dispersed into a solvent at high concentration to make a thick paste. The solution is then coated by dragging the paste across a screen placed atop the substrate. The coating is then thermally treated to evaporate solvent and remove organic ligands [69].

Screen printing is well known in the PV field. It has been used in fabricating crystalline silicon PVs, which proved to be a fiscally advantageous innovation [1]. The best cell efficiency discussed in [69] was 0.49%, but the advantages — being cost-effective, scalable, well-known to industry, and relatively simplistic — of using such a process as screen printing have proven effective in PV fabrication in the past, and could prove to be so for the CZTS material system as well in the future.

Chemical Bath Deposition:

Chemical bath deposition (CBD) is a similar process to electrodeposition. It is another non-vacuum, conceptually simple method of thin film deposition. The process depends simply on the either chemical and/or thermal dissolution and deposition of precursors based on the solution bath chemistry and the surface of the substrate [103] (fig. 2.4.5).

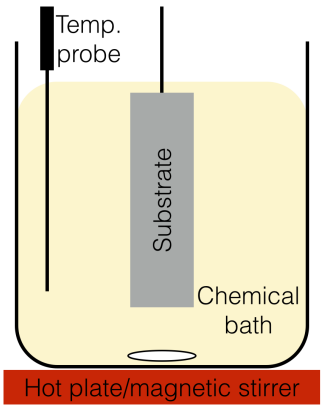

Figure 2.4.5: General schematic for a CBD setup.

CBD has been used to synthesize CZTS thin films in various ways. Wangperawong *et al* deposited copper, zinc, tin, and sulfur layers and annealed the samples to form CZTS [71]. Similar results have also been achieved by depositing layers of copper, zinc, and/or tin binary sulfides [73-75]. This method has not been shown to be viable relative to other low-cost non-vacuum based methods, with the highest efficiency reported for a CBD-deposited CZTS-based PV as 0.16% [71].

2.5: Spray Pyrolysis Synthesis of CZTS Thin Films

Aerosol spray pyrolysis is a non-vacuum solution/gas phase process. In theory, it is similar to the previously discussed solution-based processes in section 2.4.

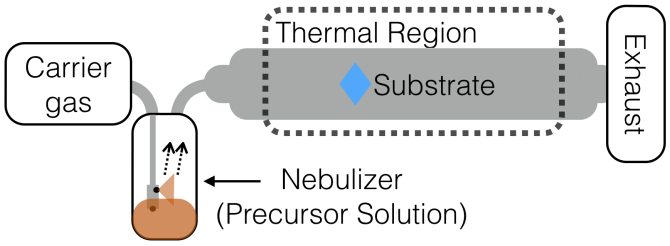

Figure 2.5.1: General schematic for a thin film aerosol spray pyrolysis setup.

Spray pyrolysis relies on the thermal decomposition of precursors in order to form a desired material. It differs, though, in the notion that the precursor solution is aerosolized via a nebulizer into micro-scale droplets before deposition to decrease the deposition speed, which theoretically allows more complete thermal equilibration to form the desired material [104] (fig. 2.5.1).

There have been several reports of using spray pyrolysis to synthesize CZTS thin films. Generally, a precursor solution containing copper, zinc, and tin chlorides or acetates plus thiourea is used, with an operating substrate temperature between 400-450

ºC [90-98]. The generally universal conclusion is that the resulting film is not phase-pure, with primarily copper sulfide impurities, and further the crystallinity of the sprayed films post-annealing is poor for PV applications.

A further disadvantage of this work is the use of metal chlorides or acetates as precursors. The chlorine or oxygen present in the precursors leads to a high concentration of undesirable impurities in the sprayed film.

Aerosol spray pyrolysis is regarded as a readily scalable method for CZTS synthesis, as it is a process well known to be successful in synthesizing nanoparticles. For example the method is used to form titania nanoparticles [105], which are commonly used in pigments and cosmetics, as well as other more technological applications.

In our work, we have studied the growth of CZTS thin films by spray pyrolysis, though we use copper, zinc, and tin diethyldithiocarbamate ($C_5H_{10}NS_2$) precursors [106]. The advantage of using these precursors is the lack of chlorine or oxygen in the ligand, which lead to impurities in the film.

2.6: CZTS Nanoparticle Synthesis

A method of creating CZTS that has been steadily growing in interest in recent years is nanoparticle sintering. It is thought to be among the most cost-effective and scalable methods outlined in this document, and marked recent improvements in reported efficiencies for nanoparticle CZTS-based PVs suggest there is still room for improvement in material processing. CZTS nanoparticle-based PVs have been reported to have 3.6%

efficiency under conventional construction [84], and up to 5.02% efficiency with a novel three-dimensional architecture [82], which puts it close the the range of PVs fabricated with vacuum-processed CZTS.

There are different methods of CZTS nanoparticle synthesis that have been employed, which yield nanoparticles with different material properties. The most common method is solution-phase thermolysis [76-79, 81-89]. In this method, precursor solutes are dissolved with the help of an acidic solvent. Typically precursor solutes are basic copper, tin, and zinc chlorides or acetates plus thiourea as the sulfur source, as are used in other solution-phase processes outlined above [76, 77, 81-86, 88, 89]. Other work has used the single-source metal and sulfur precursors copper, tin, and zinc diethyldithiocarbamates ($C_5H_{10}SN_2$) [78, 79, 87]. The advantage to the single-source metal and sulfur precursors lies in the reduction of undesirable impurity atoms in the reactor, which are present with the use of chlorides or acetates. The solution is then combined with a hot amine solvent and thermally treated under an inert atmosphere to decompose the solutes and form CZTS nanoparticles. The resultant particles are invariably capped by organic ligands leftover from the amine solvent.

The nanoparticles synthesized in the method above are highly controllable in composition and size, both ideal for adjusting the synthesis for optimal PV performance. Once the nanoparticles are isolated, they can be dispersed into a colloidal ink, then coated on a substrate. The porous nanocrystal film must then be sintered to form large crystal grains, on the order of the thickness of the film, for the best PV characteristics [1].

The work described in this document, in Chapters 3-4, outlines a novel method of controllably forming ligand-free CZTS nanoparticles via aerosol spray pyrolysis. The method is very similar to that outlined in Section 2.5 (and fig. 2.5.1), but the substrate is removed from the thermal region and a particle collection apparatus is added beyond the thermal region to collect the synthesized nanoparticles.

2.7: CZTS Sintering/Annealing

Most of the methods of forming CZTS absorber layers for PVs listed in Sections 2.4-7 require an extra annealing/sintering step in a sulfur environment. Generally, the reason is to allow thermal equilibrium of phases and crystallinity for the film to possess the optimal PV characteristics. As discussed in Section 2.3, the two most important steps to improving CZTS as a PV absorber material is passivating and decreasing undesirable defects and improving phase stability [6].

When a metal stack or metal-alloy is deposited on a substrate, the sulfur annealing process is required to diffuse sulfur into the metal layer(s) and form crystalline CZTS. The annealing time is understandably lengthy in this case, on the scale of 8-10 hours [1], in order to allow the sulfur to fully diffuse through the film and to achieve equilibrium. With sulfur already included in the pre-annealed film, the annealing step requires much less time, now on the order of 1 hour or less [1]. In this case, the annealing step is geared towards increasing crystal grain size and phase purity. With a nanoparticle CZTS film,

the annealing step is also short and aimed at increasing crystal grain size, as the nanoparticles are already assumed to be phase pure.

The conditions of the annealing process must be optimized with the CZTS film. It has been observed that under different annealing conditions, primarily with annealing temperature and sulfur pressure varied, different material phases tend to out-diffuse from the CZTS film, primarily the binary copper sulfide and tin sulfide phases [107]. The same has been observed in annealing tin-rich and copper-rich samples in our work. Typically, the stoichiometry of the film must be compensated slightly to account for the loss of some tin and copper during annealing [1].

There are two methods of sulfur-annealing used in literature. The first requires an evacuated quartz ampoule or graphite vessel with solid sulfur placed inside with the sample ([78], for example). Upon thermal treatment, the sulfur is vaporized to provide an easily variable sulfur pressure during the anneal. The other method uses a thermal flow reactor, with the sample placed inside a thermal region feeling a flow of 1-5% H_2S + 95-99% inert gas ([21], for example). Both methods have been demonstrated as effective in annealing and sintering CZTS films for use in PV cells.

2.8: CZTS Thin Film and Nanoparticle Characterization

As difficult as fabricating the complex quaternary CZTS is, characterizing the presence of phase-pure CZTS is equally challenging. X-ray diffraction (XRD), is the most common and straightforward method of characterizing crystalline phases in bulk or

nanostructured material, but XRD alone is not enough to adequately characterize CZTS. The diffraction peaks associated with kesterite CZTS are also common to other binary or ternary sulfide phases that can segregate from CZTS. In particular, zinc sulfide and copper-tin-sulfide give identical or effectively identical diffraction spectra, making it impossible to tell which phases might be present. Raman spectroscopy (Raman) in combination with XRD provides enough data to characterize each of these binary or ternary sulfide phases as separate from the quaternary kesterite CZTS phase [108].

Further material characterization can be performed via X-ray photoelectron spectroscopy (XPS) and energy dispersive x ray spectroscopy (EDS). These techniques make it possible to identify relative atomic proportions within a sample, as well as the presence and abundance of impurity elements relative to the CZTS material [29].

Optical characterization techniques also allow the identification of the semiconducting properties of a CZTS thin film or nanoparticles. Conducting UV/Vis/NIR spectrophotometry (photospec.) allows the measurement of the material's absorbance across a broad spectrum. Typically PV absorbers such as CZTS are optimized to have broad absorbance across the UV and visible spectrum, correlating to the spectrum of light given off by our sun. From this data, a Tauc plot can be created, by plotting the square of the product of the material's absorbance and the photon energy ($h\nu$) [1]. Extrapolation of the Tauc plot allows for a reasonable estimation of the materials optical band gap.

2.9: References

[1] Jiang, Minlin, and Xingzhong Y. “Cu2ZnSnS4 Thin Film Solar Cells: Present Status and Future Prospects.” In Solar Cells - Research and Application Perspectives, edited by Arturo Morales-Acevedo. InTech, 2013. <http://www.intechopen.com/books/solar-cells-research-and-application-perspectives/cu2znsns4-thin-film-solar-cells-present-status-and-future-prospects>.

[2] Green, Martin A., Keith Emery, Yoshihiro Hishikawa, Wilhelm Warta, and Ewan D. Dunlop. “Solar Cell Efficiency Tables (Version 45).” Progress in Photovoltaics: Research and Applications 23, no. 1 (January 1, 2015): 1–9. doi:10.1002/pip.2573.

[3] Fukano, Tatsuo, Shin Tajima, and Tadayoshi Ito. “Enhancement of Conversion Efficiency of Cu2ZnSnS4 Thin Film Solar Cells by Improvement of Sulfurization Conditions.” Applied Physics Express 6, no. 6 (June 1, 2013): 062301. doi:10.7567/APEX.6.062301.

[4] Wischmann, W., R. Menner, E. Lotter, R. Würz, W. Witte, S. Paetel, D. Hariskos, P. Jackson, and M. Powalla. “CIGS Thin-Film Solar Cells with an Improved Efficiency of 20.8%.” 29th European Photovoltaic Solar Energy Conference and Exhibition, November 7, 2014, 1–22.

[5] Wang, Wei, Mark T. Winkler, Oki Gunawan, Tayfun Gokmen, Teodor K. Todorov, Yu Zhu, and David B. Mitzi. “Device Characteristics of CZTSSe Thin-Film Solar Cells with 12.6% Efficiency.” Advanced Energy Materials 4, no. 7 (2014): n/a – n/a. doi:10.1002/aenm.201301465.

[6] Polizzotti, Alex, Ingrid L. Repins, Rommel Noufi, Su-Huai Wei, and David B. Mitzi. “The State and Future Prospects of Kesterite Photovoltaics.” Energy & Environmental Science 6, no. 11 (October 18, 2013): 3171–82. doi:10.1039/C3EE41781F.

[7] Mousel, Marina, Torsten Schwarz, Rabie Djemour, Thomas P. Weiss, Jan Sendler, João C. Malaquias, Alex Redinger, Oana Cojocaru-Mirédin, Pyuck-Pa Choi, and Susanne Siebentritt. “Cu-Rich Precursors Improve Kesterite Solar Cells.” Advanced Energy Materials 4, no. 2 (2014): n/a – n/a. doi:10.1002/aenm.201300543.

[8] Gershon, Talia, Tayfun Gokmen, Oki Gunawan, Richard Haight, Supratik Guha, and Byungha Shin. “Understanding the Relationship between Cu2ZnSn(S,Se)4 Material Properties and Device Performance.” MRS Communications 4, no. 04 (2014): 159–70. doi:10.1557/mrc.2014.34.

[9] Sarker, Pranab, Mowafak M. Al-Jassim, and Muhammad N. Huda. “Theoretical Limits on the Stability of Single-Phase Kesterite-Cu2ZnSnS4.” Journal of Applied Physics 117, no. 3 (January 21, 2015): 035702. doi:10.1063/1.4906065.

[10] Redinger, Alex, Dominik M. Berg, Phillip J. Dale, and Susanne Siebentritt. “The Consequences of Kesterite Equilibria for Efficient Solar Cells.” Journal of the American Chemical Society 133, no. 10 (March 16, 2011): 3320–23. doi:10.1021/ja111713g.

[11] Han, Dong, Y. Y. Sun, Junhyeok Bang, Y. Y. Zhang, Hong-Bo Sun, Xian-Bin Li, and S. B. Zhang. “Deep Electron Traps and Origin of ‘p’-Type Conductivity in the Earth-Abundant Solar-Cell Material Cu_2ZnSnS_4.” Physical Review B 87, no. 15 (April 15, 2013): 155206. doi:10.1103/PhysRevB.87.155206.

[12] Tanaka, Tooru, Akihiro Yoshida, Daisuke Saiki, Katsuhiko Saito, Qixin Guo, Mitsuhiro Nishio, and Toshiyuki Yamaguchi. “Influence of Composition Ratio on Properties of Cu2ZnSnS4 Thin Films Fabricated by Co-Evaporation.” Thin Solid Films, The 10th International Symposium on Sputtering and Plasma Processes (ISSP2009), 518, no. 21, Supplement (August 31, 2010): S29–33. doi:10.1016/j.tsf.2010.03.026.

[13] Johnson, M., S. V. Baryshev, E. Thimsen, M. Manno, X. Zhang, I. V. Veryovkin, C. Leighton, and E. S. Aydil. “Alkali-Metal-Enhanced Grain Growth in Cu2ZnSnS4 Thin Films.” Energy & Environmental Science 7, no. 6 (May 22, 2014): 1931–38. doi: 10.1039/C3EE44130J.

[14] Dasgupta, Uttiya, Sudip K. Saha, and Amlan J. Pal. “Plasmonic Effect in Pn-Junction Solar Cells Based on Layers of Semiconductor Nanocrystals: Where to Introduce Metal Nanoparticles?” Solar Energy Materials and Solar Cells 136 (May 2015): 106–12. doi:10.1016/j.solmat.2015.01.004.

[15] Kim, Hong Tak, Chang-Duk Kim, Chan Kim, Maeng Jun Kim, and Chinho Park. “Effect of Sodium Chloride (NaCl) as Crystallization Catalyst on Cu2ZnSnS4 (CZTS) Films Deposited by Wet-Solution Coating Method.” Molecular Crystals and Liquid Crystals 602, no. 1 (October 13, 2014): 144–50. doi:10.1080/15421406.2014.944754.

[16] Guijarro, Néstor, Mathieu S. Prévot, and Kevin Sivula. “Enhancing the Charge Separation in Nanocrystalline Cu2ZnSnS4 Photocathodes for Photoelectrochemical Application: The Role of Surface Modifications.” The Journal of Physical Chemistry Letters 5, no. 21 (2014): 3902–8. doi:10.1021/jz501996s.

[17] Baryshev, Sergey V., and Elijah Thimsen. “Enthalpy of Formation for Cu–Zn–Sn–S (CZTS) Calculated from Surface Binding Energies Experimentally Measured by Ion Sputtering.” Chemistry of Materials, March 11, 2015. doi:10.1021/cm504749d.

[18] Shin, Byungha, Yu Zhu, Nestor A. Bojarczuk, S. Jay Chey, and Supratik Guha. “Control of an Interfacial MoSe2 Layer in Cu2ZnSnSe4 Thin Film Solar Cells: 8.9% Power Conversion Efficiency with a TiN Diffusion Barrier.” Applied Physics Letters 101, no. 5 (July 30, 2012): 053903. doi:10.1063/1.4740276.

[19] Haque, F., N.A. Khan, K.S. Rahman, M.A. Islam, M.M. Alam, K. Sopian, and N. Amin. “Prospects of Zinc Sulphide as an Alternative Buffer Layer for CZTS Solar Cells from Numerical Analysis.” In 2014 International Conference on Electrical and Computer Engineering (ICECE), 504–7, 2014. doi:10.1109/ICECE.2014.7026855.

[20] Yu, Kin Man, Marie A. Mayer, Derrick T. Speaks, Hongcai He, Ruying Zhao, L. Hsu, Samuel S. Mao, E. E. Haller, and Wladek Walukiewicz. “Ideal Transparent Conductors for Full Spectrum Photovoltaics.” Journal of Applied Physics 111, no. 12 (June 15, 2012): 123505. doi:10.1063/1.4729563.

[21] Katagiri, H., N. Sasaguchi, S. Hando, J. Ohashi, S. Hoshino, and T. Yokota. “Preparation and Evaluation of Cu2ZnSnS4 Thin Films by Sulfurization of E-B Evaporated Precursors.” Solar Energy Materials and Solar Cells 49, no. 1 (December 1, 1997): 407–14. doi:10.1016/S0927-0248(97)00119-0.

[22] Araki, Hideaki, Aya Mikaduki, Yuki Kubo, Tatsuhiro Sato, Kazuo Jimbo, Win Shwe Maw, Hironori Katagiri, Makoto Yamazaki, Koichiro Oishi, and Akiko Takeuchi. “Preparation of Cu2ZnSnS4 Thin Films by Sulfurization of Stacked Metallic Layers.” Thin Solid Films, Proceedings of 2nd International Symposium on the Manipulation of Advanced Smart Materials, 517, no. 4 (December 31, 2008): 1457–60. doi:10.1016/j.tsf.2008.09.058.

[23] Katagiri, Hironori, Naoya Ishigaki, Takeshi Ishida, and Kotoe Saito. “Characterization of Cu2ZnSnS4 Thin Films Prepared by Vapor Phase Sulfurization.” Japanese Journal of Applied Physics 40, no. 2R (February 1, 2001): 500. doi:10.1143/JJAP.40.500.

[24] Kobayashi, Takeshi, Kazuo Jimbo, Kazuyuki Tsuchida, Shunsuke Shinoda, Taisuke Oyanagi, and Hironori Katagiri. “Investigation of Cu2ZnSnS4-Based Thin Film Solar Cells Using Abundant Materials.” Japanese Journal of Applied Physics 44, no. 1S (January 1, 2005): 783. doi:10.1143/JJAP.44.783.

[25] Schubert, Björn-Arvid, Björn Marsen, Sonja Cinque, Thomas Unold, Reiner Klenk, Susan Schorr, and Hans-Werner Schock. “Cu2ZnSnS4 Thin Film Solar Cells by Fast Coevaporation.” Progress in Photovoltaics: Research and Applications 19, no. 1 (January 1, 2011): 93–96. doi:10.1002/pip.976.

[26] Weber, A., H. Krauth, S. Perlt, B. Schubert, I. Kötschau, S. Schorr, and H. W. Schock. “Multi-Stage Evaporation of Cu2ZnSnS4 Thin Films.” Thin Solid Films, Thin Film Chalogenide Photovoltaic Materials (EMRS, Symposium L), 517, no. 7 (February 2, 2009): 2524–26. doi:10.1016/j.tsf.2008.11.033.

[27] Wang, K., O. Gunawan, T. Todorov, B. Shin, S. J. Chey, N. A. Bojarczuk, D. Mitzi, and S. Guha. “Thermally Evaporated Cu2ZnSnS4 Solar Cells.” Applied Physics Letters 97 (October 1, 2010): 143508. doi:10.1063/1.3499284.

[28] Shin, Byungha, Yu Zhu, Talia Gershon, Nestor A. Bojarczuk, and Supratik Guha. “Epitaxial Growth of Kesterite Cu2ZnSnS4 on a Si(001) Substrate by Thermal Co-Evaporation.” Thin Solid Films 556 (April 1, 2014): 9–12. doi:10.1016/j.tsf.2013.12.046.

[29] Hurtado, M., S.D. Cruz, R.A. Becerra, C. Calderon, P. Bartolo-Perez, and G. Gordillo. “XPS Analysis and Structural Characterization of CZTS Thin Films Prepared Using Solution and Vacuum Based Deposition Techniques.” In Photovoltaic Specialist Conference (PVSC), 2014 IEEE 40th, 0368–72, 2014. doi:10.1109/PVSC.2014.6924934.

[30] Li, Ye, Junfang Chen, and Junhui Ma. “Properties of Cu2ZnSnS4 (CZTS) Thin Films Prepared by Plasma Assisted Co-Evaporation.” Journal of Materials Science: Materials in Electronics, June 3, 2015, 1–6. doi:10.1007/s10854-015-3251-5.

[31] Zhang, Jie, Bo Long, Shuying Cheng, and Weibo Zhang. “Effects of Sulfurization Temperature on Properties of CZTS Films by Vacuum Evaporation and Sulfurization Method.” International Journal of Photoenergy 2013 (October 9, 2013): e986076. doi: 10.1155/2013/986076.

[32] Shin, Byungha, Oki Gunawan, Yu Zhu, Nestor A. Bojarczuk, S. Jay Chey, and Supratik Guha. “Thin Film Solar Cell with 8.4% Power Conversion Efficiency Using an Earth-Abundant Cu2ZnSnS4 Absorber.” Progress in Photovoltaics: Research and Applications 21, no. 1 (January 1, 2013): 72–76. doi:10.1002/pip.1174.

[33] Ito, Kentaro, and Tatsuo Nakazawa. “Electrical and Optical Properties of Stannite-Type Quaternary Semiconductor Thin Films.” Japanese Journal of Applied Physics 27, no. 11R (November 1, 1988): 2094. doi:10.1143/JJAP.27.2094.

[34] Hyesun Yoo, JunHo Kim. “Comparative Study of Cu2ZnSnS4 Film Growth.” Solar Energy Materials and Solar Cells 95, no. 1 (2011): 239–44. doi:10.1016/j.solmat.2010.04.060.

[35] Zhang, Jun, and LeXi Shao. “Cu2ZnSnS4 Thin Films Prepared by Sulfurizing Different Multilayer Metal Precursors.” Science in China Series E: Technological Sciences 52, no. 1 (January 14, 2009): 269–72. doi:10.1007/s11431-009-0013-8.

[36] Jimbo, Kazuo, Ryoichi Kimura, Tsuyoshi Kamimura, Satoru Yamada, Win Shwe Maw, Hideaki Araki, Koichiro Oishi, and Hironori Katagiri. “Cu2ZnSnS4-Type Thin Film Solar Cells Using Abundant Materials.” Thin Solid Films, Proceedings of Sympodium O on Thin Film Chalcogenide Photovoltaic Materials, EMRS 2006 ConferenceEMRS 2006 Symposium O, 515, no. 15 (May 31, 2007): 5997–99. doi:10.1016/j.tsf.2006.12.103.

[37] Katagiri, Hironori, Kazuo Jimbo, Satoru Yamada, Tsuyoshi Kamimura, Win Shwe Maw, Tatsuo Fukano, Tadashi Ito, and Tomoyoshi Motohiro. “Enhanced Conversion Efficiencies of Cu2ZnSnS4-Based Thin Film Solar Cells by Using Preferential Etching Technique.” Applied Physics Express 1, no. 4 (April 1, 2008): 041201. doi:10.1143/APEX.1.041201.

[38] Liu, Fangyang, Yi Li, Kun Zhang, Bo Wang, Chang Yan, Yanqing Lai, Zhian Zhang, Jie Li, and Yexiang Liu. “In Situ Growth of Cu2ZnSnS4 Thin Films by Reactive Magnetron Co-Sputtering.” Solar Energy Materials and Solar Cells 94, no. 12 (December 2010): 2431–34. doi:10.1016/j.solmat.2010.08.003.

[39] Dhakal, Tara P., Chien–Yi Peng, R. Reid Tobias, Ramesh Dasharathy, and Charles R. Westgate. “Characterization of a CZTS Thin Film Solar Cell Grown by Sputtering Method.” Solar Energy 100 (February 2014): 23–30. doi:10.1016/j.solener.2013.11.035.

[40] Katagiri, Hironori, Kazuo Jimbo, and Tsukasa Washio. “Development of Earth-Abundant CZTS Thin Film Solar Cells with Sulfurization Technique.” In Symposium E/H – Advances in the Characterization, Performance and Defect Engineering of Earth Abundant and Thin-Film Materials for Solar Energy Conversion, Vol. 1670. MRS Online Proceedings Library, 2014. doi:10.1557/opl.2014.851.

[41] Muhunthan, N., Om Pal Singh, Son Singh, and V. N. Singh. “Growth of CZTS Thin Films by Cosputtering of Metal Targets and Sulfurization in H2S.” International Journal of Photoenergy 2013 (August 6, 2013): e752012. doi:10.1155/2013/752012.

[42] Inamdar, A. I., Seulgi Lee, Ki-Young Jeon, Chong Ha Lee, S. M. Pawar, R. S. Kalubarme, Chan Jin Park, Hyunsik Im, Woong Jung, and Hyungsang Kim. “Optimized Fabrication of Sputter Deposited Cu2ZnSnS4 (CZTS) Thin Films.” Solar Energy 91 (May 2013): 196–203. doi:10.1016/j.solener.2013.02.003.

[43] Wang, Jiansheng, Song Li, Jiajia Cai, Bo Shen, Yuping Ren, and Gaowu Qin. “Cu2ZnSnS4 Thin Films: Facile and Cost-Effective Preparation by RF-Magnetron Sputtering and Texture Control.” Journal of Alloys and Compounds 552 (March 5, 2013): 418–22. doi:10.1016/j.jallcom.2012.11.082.

[44] Zhou, Shanshan, Ruiqin Tan, Xin Jiang, Xiang Shen, Wei Xu, and Weijie Song. “Growth of CZTS Thin Films by Sulfurization of Sputtered Single-Layered Cu–Zn–Sn Metallic Precursors from an Alloy Target.” Journal of Materials Science: Materials in Electronics 24, no. 12 (October 13, 2013): 4958–63. doi:10.1007/s10854-013-1507-5.

[45] Amal, Muhamad I., and Kyoo Ho Kim. “Crystallization of Kesterite Cu2ZnSnS4 Prepared by the Sulfurization of Sputtered Cu–Zn–Sn Precursors.” Thin Solid Films 534 (May 1, 2013): 144–48. doi:10.1016/j.tsf.2013.02.028.

[46] Ahmed, Shafaat, Kathleen B. Reuter, Oki Gunawan, Lian Guo, Lubomyr T. Romankiw, and Hariklia Deligianni. “A High Efficiency Electrodeposited Cu2ZnSnS4 Solar Cell.” Advanced Energy Materials 2, no. 2 (February 1, 2012): 253–59. doi: 10.1002/aenm.201100526.

[47] Scragg, Jonathan J., Philip J. Dale, Laurence M. Peter, Guillaume Zoppi, and Ian Forbes. “New Routes to Sustainable Photovoltaics: Evaluation of Cu2ZnSnS4 as an Alternative Absorber Material.” Physica Status Solidi (b) 245, no. 9 (September 1, 2008): 1772–78. doi:10.1002/pssb.200879539.

[48] Pawar, S. M., B. S. Pawar, A. V. Moholkar, D. S. Choi, J. H. Yun, J. H. Moon, S. S. Kolekar, and J. H. Kim. “Single Step Electrosynthesis of Cu2ZnSnS4 (CZTS) Thin Films for Solar Cell Application.” Electrochimica Acta 55, no. 12 (April 30, 2010): 4057–61. doi:10.1016/j.electacta.2010.02.051.

[49] Araki, Hideaki, Yuki Kubo, Aya Mikaduki, Kazuo Jimbo, Win Shwe Maw, Hironori Katagiri, Makoto Yamazaki, Koichiro Oishi, and Akiko Takeuchi. “Preparation of

Cu2ZnSnS4 Thin Films by Sulfurizing Electroplated Precursors." Solar Energy Materials and Solar Cells, 17th International Photovoltaic Science and Engineering Conference, 93, no. 6–7 (June 2009): 996–99. doi:10.1016/j.solmat.2008.11.045.

[50] Gurav, K. V., S. W. Shin, U. M. Patil, M. P. Suryawanshi, S. M. Pawar, M. G. Gang, S. A. Vanalakar, J. H. Yun, and J. H. Kim. "Improvement in the Properties of CZTSSe Thin Films by Selenizing Single-Step Electrodeposited CZTS Thin Films." Journal of Alloys and Compounds 631 (May 15, 2015): 178–82. doi:10.1016/j.jallcom.2014.12.253.

[51] Chen, Hao, Qinyan Ye, Xulin He, Jingjing Ding, Yongzheng Zhang, Junfeng Han, Jiang Liu, Cheng Liao, Jun Mei, and Woonming Lau. "Electrodeposited CZTS Solar Cells from Reline Electrolyte." Green Chemistry 16, no. 8 (July 21, 2014): 3841–45. doi: 10.1039/C4GC00142G.

[52] Lee, Seul Gi, Jongmin Kim, Huyn Suk Woo, Yongcheol Jo, A. I. Inamdar, S. M. Pawar, Hyung Sang Kim, Woong Jung, and Hyun Sik Im. "Structural, Morphological, Compositional, and Optical Properties of Single Step Electrodeposited Cu2ZnSnS4 (CZTS) Thin Films for Solar Cell Application." Current Applied Physics 14, no. 3 (March 2014): 254–58. doi:10.1016/j.cap.2013.11.028.

[53] Jeon, Minsung, Tomohiro Shimizu, and Shoso Shingubara. "Cu2ZnSnS4 Thin Films and Nanowires Prepared by Different Single-Step Electrodeposition Method in Quaternary Electrolyte." Materials Letters 65, no. 15–16 (August 2011): 2364–67. doi: 10.1016/j.matlet.2011.05.003.

[54] Tanaka, Kunihiko, Masatoshi Oonuki, Noriko Moritake, and Hisao Uchiki. "Thin Film Solar Cells Prepared by Non-Vacuum Processing." Solar Energy Materials and Solar Cells 93, no. 5 (May 2009): 583–87. doi:10.1016/j.solmat.2008.12.009.

[55] Tanaka, Kunihiko, Yuki Fukui, Noriko Moritake, and Hisao Uchiki. "Chemical Composition Dependence of Morphological and Optical Properties of Cu2ZnSnS4 Thin Films Deposited by Sol–gel Sulfurization and Cu2ZnSnS4 Thin Film Solar Cell Efficiency." Solar Energy Materials and Solar Cells 95, no. 3 (March 2011): 838–42. doi: 10.1016/j.solmat.2010.10.031.

[56] Su, Zhenghua, Kaiwen Sun, Zili Han, Hongtao Cui, Fangyang Liu, Yanqing Lai, Jie Li, Xiaojing Hao, Yexiang Liu, and Martin A. Green. "Fabrication of Cu2ZnSnS4 Solar Cells with 5.1% Efficiency via Thermal Decomposition and Reaction Using a Non-Toxic Sol–gel Route." Journal of Materials Chemistry A 2, no. 2 (December 3, 2013): 500–509. doi:10.1039/C3TA13533K.

[57] Park, Hyungjin, Young Hwan Hwang, and Byeong-Soo Bae. “Sol–gel Processed Cu2ZnSnS4 Thin Films for a Photovoltaic Absorber Layer without Sulfurization.” Journal of Sol-Gel Science and Technology 65, no. 1 (February 7, 2012): 23–27. doi: 10.1007/s10971-012-2703-0.

[58] Kahraman, S., S. Çetinkaya, H. A. Çetinkara, and H. S. Güder. “A Comparative Study of Cu2ZnSnS4 Thin Films Growth by Successive Ionic Layer Adsorption–reaction and Sol-Gel Methods.” Thin Solid Films 550 (January 1, 2014): 36–39. doi:10.1016/j.tsf. 2013.10.035.

[59] Zhao, Wangen, Gang Wang, Qingwen Tian, Yanchun Yang, Lijian Huang, and Daocheng Pan. “Fabrication of Cu2ZnSn(S,Se)4 Solar Cells via an Ethanol-Based Sol–Gel Route Using SnS2 as Sn Source.” ACS Applied Materials & Interfaces 6, no. 15 (August 13, 2014): 12650–55. doi:10.1021/am5026006.

[60] Chaudhuri, Tapas Kumar, and Devendra Tiwari. “Earth-Abundant Non-Toxic Cu2ZnSnS4 Thin Films by Direct Liquid Coating from Metal–thiourea Precursor Solution.” Solar Energy Materials and Solar Cells 101 (June 2012): 46–50. doi:10.1016/ j.solmat.2012.02.012.

[61] Mitzi, David B., Oki Gunawan, Teodor K. Todorov, Kejia Wang, and Supratik Guha. “The Path towards a High-Performance Solution-Processed Kesterite Solar Cell.” Special Issue : Thin Film and Nanostructured Solar Cells 95, no. 6 (June 2011): 1421–36. doi: 10.1016/j.solmat.2010.11.028.

[62] Agawane, G.L., A.S. Kamble, S.A. Vanalakar, S.W. Shin, M.G. Gang, Jae Ho Yun, Jihye Gwak, A.V. Moholkar, and Jin Hyeok Kim. “Fabrication of 3.01% Power Conversion Efficient High-Quality CZTS Thin Film Solar Cells by a Green and Simple Sol–gel Technique.” Materials Letters 158 (November 1, 2015): 58–61. doi:10.1016/ j.matlet.2015.05.036.

[63] Moriya, Katsuhiko, Kunihiko Tanaka, and Hisao Uchiki. “Cu2ZnSnS4 Thin Films Annealed in H2S Atmosphere for Solar Cell Absorber Prepared by Pulsed Laser Deposition.” Japanese Journal of Applied Physics 47, no. 1S (January 1, 2008): 602. doi: 10.1143/JJAP.47.602.

[64] Moholkar, A. V., S. S. Shinde, A. R. Babar, Kyu-Ung Sim, Ye-bin Kwon, K. Y. Rajpure, P. S. Patil, C. H. Bhosale, and J. H. Kim. “Development of CZTS Thin Films

Solar Cells by Pulsed Laser Deposition: Influence of Pulse Repetition Rate." Solar Energy 85, no. 7 (July 2011): 1354–63. doi:10.1016/j.solener.2011.03.017.

[65] Moriya, Katsuhiko, Kunihiko Tanaka, and Hisao Uchiki. "Fabrication of Cu2ZnSnS4 Thin-Film Solar Cell Prepared by Pulsed Laser Deposition." Japanese Journal of Applied Physics 46, no. 9R (September 1, 2007): 5780. doi:10.1143/JJAP.46.5780.

[66] Crovetto, Andrea, Andrea Cazzaniga, Rebecca B. Ettlinger, Jørgen Schou, and Ole Hansen. "Optical Properties and Surface Characterization of Pulsed Laser-Deposited Cu2ZnSnS4 by Spectroscopic Ellipsometry." Thin Solid Films, E-MRS 2014 Spring Meeting, Symposium A, Thin-Film Chalcogenide Photovoltaic Materials, 582 (May 1, 2015): 203–7. doi:10.1016/j.tsf.2014.11.075.

[67] Che Sulaiman, Nurul Suhada, Chen Hon Nee, Seong Ling Yap, Yen Sian Lee, Teck Yong Tou, and Seong Shan Yap. "The Growth of Nanostructured Cu2ZnSnS4 Films by Pulsed Laser Deposition." Applied Surface Science. Accessed August 1, 2015. doi:10.1016/j.apsusc.2015.02.096.

[68] Ettlinger, Rebecca Bolt, Andrea Cazzaniga, Stela Canulescu, Nini Pryds, and Jørgen Schou. "Pulsed Laser Deposition from ZnS and Cu2SnS3 Multicomponent Targets." E-MRS 2014 Spring Meeting. Symposium J. Laser Interaction with Advanced Materials: Fundamentals and Applications 336 (May 1, 2015): 385–90. doi:10.1016/j.apsusc.2014.12.165.

[69] Zhou, Zhihua, Yanyan Wang, Dong Xu, and Yafei Zhang. "Fabrication of Cu2ZnSnS4 Screen Printed Layers for Solar Cells." Solar Energy Materials and Solar Cells 94, no. 12 (December 2010): 2042–45. doi:10.1016/j.solmat.2010.06.010.

[70] Dai, Pengcheng, Yanhe Zhang, Yanming Xue, Xiangfen Jiang, Xuebin Wang, Jinhua zhan, and Yoshio Bando. "Nanoparticle-Based Screen Printing of Copper Zinc Tin Sulfide Thin Film as Photocathode for Quantum Dot Sensitized Solar Cell." Materials Letters 158 (November 1, 2015): 198–201. doi:10.1016/j.matlet.2015.06.016.

[71] Wangperawong, A., J. S. King, S. M. Herron, B. P. Tran, K. Pangan-Okimoto, and S. F. Bent. "Aqueous Bath Process for Deposition of Cu2ZnSnS4 Photovoltaic Absorbers." Thin Solid Films 519, no. 8 (February 1, 2011): 2488–92. doi:10.1016/j.tsf.2010.11.040.

[72] Mali, Sawanta S., Pravin S. Shinde, Chirayath A. Betty, Popatrao N. Bhosale, Young Woo Oh, and Pramod S. Patil. "Synthesis and Characterization of Cu2ZnSnS4 Thin Films

by SILAR Method." Journal of Physics and Chemistry of Solids 73, no. 6 (June 2012): 735–40. doi:10.1016/j.jpcs.2012.01.008.

[73] Gao, Chao, Honglie Shen, Feng Jiang, and Hao Guan. "Preparation of Cu2ZnSnS4 Film by Sulfurizing Solution Deposited Precursors." Applied Surface Science 261 (November 15, 2012): 189–92. doi:10.1016/j.apsusc.2012.07.137.

[74] Suarez, H., J.M. Correa, S.D. Cruz, C.A. Otalora, M. Hurtado, and G. Gordillo. "Synthesis and Study of Properties of CZTS Thin Films Grown Using a Novel Solution-Based Chemical Route." In Photovoltaic Specialists Conference (PVSC), 2013 IEEE 39th, 2585–89, 2013. doi:10.1109/PVSC.2013.6745002.

[75] Li, Jianmin, Yaguang Wang, Guoshun Jiang, Weifeng Liu, and Changfei Zhu. "Cu2MSnS4 (M: Zn, Cd, Mn) Thin Films Fabricated with Stacked Layers by CBD-Annealing Route." Materials Letters 157 (October 15, 2015): 27–29. doi:10.1016/j.matlet.2015.05.068.

[76] Kameyama, Tatsuya, Takaaki Osaki, Ken-ichi Okazaki, Tamaki Shibayama, Akihiko Kudo, Susumu Kuwabata, and Tsukasa Torimoto. "Preparation and Photoelectrochemical Properties of Densely Immobilized Cu2ZnSnS4 Nanoparticle Films." Journal of Materials Chemistry 20, no. 25 (2010): 5319. doi:10.1039/c0jm00454e.

[77] Guo, Qijie, Hugh W. Hillhouse, and Rakesh Agrawal. "Synthesis of Cu2ZnSnS4 Nanocrystal Ink and Its Use for Solar Cells." Journal of the American Chemical Society 131, no. 33 (2009): 11672–73. doi:10.1021/ja904981r.

[78] Chernomordik, B. D., A. E. Béland, N. D. Trejo, A. A. Gunawan, D. D. Deng, K. A. Mkhoyan, and E. S. Aydil. "Rapid Facile Synthesis of Cu2ZnSnS4 Nanocrystals." Journal of Materials Chemistry A 2, no. 27 (June 17, 2014): 10389–95. doi:10.1039/C4TA01658K.

[79] Khare, Ankur, Andrew W. Wills, Lauren M. Ammerman, David J. Norris, and Eray S. Aydil. "Size Control and Quantum Confinement in Cu2ZnSnS4 Nanocrystals." Chemical Communications 47, no. 42 (October 18, 2011): 11721–23. doi:10.1039/C1CC14687D.

[80] Park, Jongpil, Miyeon Song, Won Mok Jung, Won Young Lee, Hanggeun Kim, Youngkwon Kim, Chahwan Hwang, and Il-Wun Shim. "Syntheses of Cu2SnS3 and Cu2ZnSnS4 Nanoparticles with Tunable Zn/Sn Ratios under Multibubble

Sonoluminescence Conditions." Dalton Transactions 42, no. 29 (July 2, 2013): 10545–50. doi:10.1039/C3DT50849H.

[81] Steinhagen, Chet, Matthew G. Panthani, Vahid Akhavan, Brian Goodfellow, Bonil Koo, and Brian A. Korgel. "Synthesis of Cu2ZnSnS4 Nanocrystals for Use in Low-Cost Photovoltaics." Journal of the American Chemical Society 131, no. 35 (September 9, 2009): 12554–55. doi:10.1021/ja905922j.

[82] Park, Si-Nae, Shi-Joon Sung, Jun-Hyoung Sim, Kee-Jeong Yang, Dae-Kue Hwang, JunHo Kim, Gee Yeong Kim, William Jo, Dae-Hwan Kim, and Jin-Kyu Kang. "Nanostructured P-Type CZTS Thin Films Prepared by a Facile Solution Process for 3D P–n Junction Solar Cells." Nanoscale 7, no. 25 (June 18, 2015): 11182–89. doi:10.1039/C5NR02081F.

[83] Zhou, Huanping, Wan-Ching Hsu, Hsin-Sheng Duan, Brion Bob, Wenbing Yang, Tze-Bin Song, Chia-Jung Hsu, and Yang Yang. "CZTS Nanocrystals: A Promising Approach for next Generation Thin Film Photovoltaics." Energy & Environmental Science 6, no. 10 (September 20, 2013): 2822–38. doi:10.1039/C3EE41627E.

[84] Kim, Youngwoo, Kyoohee Woo, Inhyuk Kim, Yong Soo Cho, Sunho Jeong, and Jooho Moon. "Highly Concentrated Synthesis of Copper-Zinc-Tin-Sulfide Nanocrystals with Easily Decomposable Capping Molecules for Printed Photovoltaic Applications." Nanoscale 5, no. 21 (October 10, 2013): 10183–88. doi:10.1039/C3NR03104G.

[85] Collord, Andrew D., and Hugh W. Hillhouse. "Composition Control and Formation Pathway of CZTS and CZTGS Nanocrystal Inks for Kesterite Solar Cells." Chemistry of Materials 27, no. 5 (March 10, 2015): 1855–62. doi:10.1021/acs.chemmater.5b00104.

[86] Peng, Xiaoli, Wenbin Guo, Shu Zhang, and Yong Xiang. "Solvothermal Synthesis of Cu2ZnSnS4 Nanocrystals by Using Metal Oxides." In 2014 International Symposium on Next-Generation Electronics (ISNE), 1–2, 2014. doi:10.1109/ISNE.2014.6839335.

[87] Williams, Bryce A., Ankit Mahajan, Michelle A. Smeaton, Collin S. Holgate, Eray S. Aydil, and Lorraine F. Francis. "Formation of Copper Zinc Tin Sulfide Thin Films from Colloidal Nanocrystal Dispersions via Aerosol-Jet Printing and Compaction." ACS Applied Materials & Interfaces 7, no. 21 (June 3, 2015): 11526–35. doi:10.1021/acsami.5b02484.

[88] Dai, Pengcheng, Yanhe Zhang, Yanming Xue, Xiangfen Jiang, Xuebin Wang, Jinhua zhan, and Yoshio Bando. "Nanoparticle-Based Screen Printing of Copper Zinc Tin

Sulfide Thin Film as Photocathode for Quantum Dot Sensitized Solar Cell." Materials Letters 158 (November 1, 2015): 198–201. doi:10.1016/j.matlet.2015.06.016.

[89] Akhavan, Vahid A., Brian W. Goodfellow, Matthew G. Panthani, Chet Steinhagen, Taylor B. Harvey, C. Jackson Stolle, and Brian A. Korgel. "Colloidal CIGS and CZTS Nanocrystals: A Precursor Route to Printed Photovoltaics." Solution Processing Technology for Inorganic Films, Nanostructures and Functional Materials, Symposium JJ, 6th International Conference on Materials for Advanced Technologies, 26 June to 1 July 2011, Singapore 189 (May 2012): 2–12. doi:10.1016/j.jssc.2011.11.002.

[90] Hyesun Yoo, JunHo Kim. "Comparative Study of Cu2ZnSnS4 Film Growth." Solar Energy Materials and Solar Cells 95, no. 1 (2011): 239–44. doi:10.1016/j.solmat.2010.04.060.

[91] Kamoun, N., H. Bouzouita, and B. Rezig. "Fabrication and Characterization of Cu2ZnSnS4 Thin Films Deposited by Spray Pyrolysis Technique." Thin Solid Films, Proceedings of Sympodium O on Thin Film Chalcogenide Photovoltaic Materials, EMRS 2006 ConferenceEMRS 2006 Symposium O, 515, no. 15 (May 31, 2007): 5949–52. doi:10.1016/j.tsf.2006.12.144.

[92] Valdés, M., G. Santoro, and M. Vázquez. "Spray Deposition of Cu2ZnSnS4 Thin Films." Journal of Alloys and Compounds 585 (February 5, 2014): 776–82. doi:10.1016/j.jallcom.2013.10.009.

[93] Majeed Khan, M. A., Sushil Kumar, Mansour Alhoshan, and A. S. Al Dwayyan. "Spray Pyrolysed Cu2ZnSnS4 Absorbing Layer: A Potential Candidate for Photovoltaic Applications." Optics & Laser Technology 49 (July 2013): 196–201. doi:10.1016/j.optlastec.2012.12.012.

[94] Espindola-Rodriguez, M., M. Placidi, O. Vigil-Galán, V. Izquierdo-Roca, X. Fontané, A. Fairbrother, D. Sylla, E. Saucedo, and A. Pérez-Rodríguez. "Compositional Optimization of Photovoltaic Grade Cu2ZnSnS4 Films Grown by Pneumatic Spray Pyrolysis." Thin Solid Films 535 (May 15, 2013): 67–72. doi:10.1016/j.tsf.2012.12.082.

[95] Gurieva, G., M. Guc, L. I. Bruk, V. Izquierdo-Roca, A. Pérez Rodríguez, S. Schorr, and E. Arushanov. "Cu2ZnSnS4 Thin Films Grown by Spray Pyrolysis: Characterization by Raman Spectroscopy and X-Ray Diffraction." Physica Status Solidi (c) 10, no. 7–8 (August 1, 2013): 1082–85. doi:10.1002/pssc.201200856.

[96] Aono, Masami, Koichiro Yoshitake, and Hisashi Miyazaki. “XPS Depth Profile Study of CZTS Thin Films Prepared by Spray Pyrolysis.” Physica Status Solidi (c) 10, no. 7–8 (August 1, 2013): 1058–61. doi:10.1002/pssc.201200796.

[97] Rajeshmon, V.G., C. Sudha Kartha, K.P. Vijayakumar, C. Sanjeeviraja, T. Abe, and Y. Kashiwaba. “Role of Precursor Solution in Controlling the Opto-Electronic Properties of Spray Pyrolysed Cu2ZnSnS4 Thin Films.” Solar Energy 85, no. 2 (February 2011): 249–55. doi:10.1016/j.solener.2010.12.005.

[98] Shinde, N.M., R.J. Deokate, and C.D. Lokhande. “Properties of Spray Deposited Cu2ZnSnS4 (CZTS) Thin Films.” Journal of Analytical and Applied Pyrolysis 100 (March 2013): 12–16. doi:10.1016/j.jaap.2012.10.018.

[99] Harsha, Professor K. S. K. S. Sree. Principles of Vapor Deposition of Thin Films. Elsevier, 2005.

[100] “What Is Sputtering?” AJA International. Accessed August 4, 2015. http://www.ajaint.com/what-is-sputtering.html.

[101] Schwarzacher, Walther. “Electrodeposition: A Technology for the Future”. The Electrochemical Society. *Interface*, Spring 2006. 32-35.

[102] Krebs, Hans-Ulrich, Martin Weisheit, Jörg Faupel, Erik Süske, Thorsten Scharf, Christian Fuhse, Michael Störmer, et al. “Pulsed Laser Deposition (PLD) -- A Versatile Thin Film Technique.” In Advances in Solid State Physics, edited by Bernhard Kramer, 505–18. Advances in Solid State Physics 43. Springer Berlin Heidelberg, 2003. http://link.springer.com/chapter/10.1007/978-3-540-44838-9_36.

[103] Hodes, Gary. “Semiconductor and Ceramic Nanoparticle Films Deposited by Chemical Bath Deposition.” Physical Chemistry Chemical Physics 9, no. 18 (May 9, 2007): 2181–96. doi:10.1039/B616684A.

[104] Sorensen, C. M., Q. Li, H. K. Xu, Z. X. Tang, K. J. Klabunde, and G. C. Hadjipanayis. “Aerosol Spray Pyrolysis Synthesis Techniques.” In Nanophase Materials, edited by George C. Hadjipanayis and Richard W. Siegel, 109–16. NATO ASI Series 260. Springer Netherlands, 1994. http://link.springer.com/chapter/10.1007/978-94-011-1076-1_15.

[105] Wang, Wei-Ning, I. Wuled Lenggoro, Yoshitake Terashi, Tae Oh Kim, and Kikuo Okuyama. “One-Step Synthesis of Titanium Oxide Nanoparticles by Spray Pyrolysis of

Organic Precursors." Materials Science and Engineering: B 123, no. 3 (November 25, 2005): 194–202. doi:10.1016/j.mseb.2005.08.006.

[106] Exarhos, S., K. N. Bozhilov, and L. Mangolini. "Spray Pyrolysis of CZTS Nanoplatelets." Chemical Communications 50, no. 77 (August 28, 2014): 11366–69. doi: 10.1039/C4CC05162A.

[107] Emrani, Amin, Parag Vasekar, and Charles R. Westgate. "Effects of Sulfurization Temperature on CZTS Thin Film Solar Cell Performances." Solar Energy 98, Part C (December 2013): 335–40. doi:10.1016/j.solener.2013.09.020.

[108] Cheng, A.-J., M. Manno, A. Khare, C. Leighton, S. A. Campbell, and E. S. Aydil. "Imaging and Phase Identification of Cu2ZnSnS4 Thin Films Using Confocal Raman Spectroscopy." Journal of Vacuum Science & Technology A 29, no. 5 (September 1, 2011): 051203. doi:10.1116/1.3625249.

Chapter 3: Experimental

3.1: Precursor Synthesis

In order to ensure consistent precursor quality, the metal-diethyldithiocarbamate precursors are formed in-house. The precursor synthesis is outlined in the supplement to [1]. In essence, sodium diethyldithiocarbamate is mixed with zinc, tin, and copper chlorides to cause an ion-replacement to form sodium chloride and metal diethyldithiocarbamate products, which are then cleaned and purified to isolate the desired material.

To form zinc diethyldithiocarbamate — $Zn(dedc)_2$ — (white), 9.0 g of sodium diethyldithiocarbamate (Sigma-Aldrich Corporation, St. Louis, MO) is dissolved in 150 mL of ethanol. Concurrently, 3.38 g of zinc chloride (Sigma-Aldrich Corporation, St. Louis, MO) is dissolved in 50 mL of ethanol. The sodium diethyldithiocarbamate solution is added dropwise to the zinc chloride solution under constant stirring via a burette. Upon completion of the solution combination, the product is stirred for a further ten minutes, followed by ten minutes of ultrasonication, to ensure

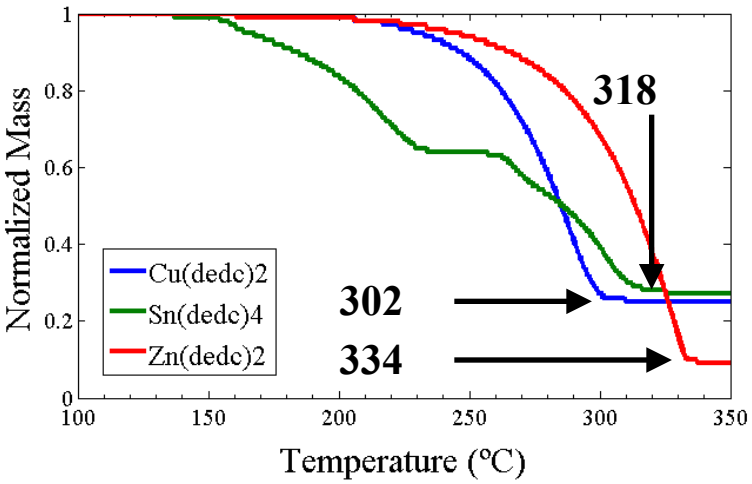

Figure 3.1.1: Shows thermogravimetric analysis and decomposition of $Zn(dedc)_2$ (red), $Sn(dedc)_4$ (green), and $Cu(dedc)_2$ (blue) with temperature.

completion of the ion-replacement reaction. The product is then washed in ethanol and deionized water, separated via centrifuge, and washed again until the product is washed five times. The product is then dissolved in chloroform and dried under argon flow. The synthesized $Zn(dedc)_2$ is fully decomposed above 334 ºC (fig. 3.1.1).

To form tin diethyldithiocarbamate — $Sn(dedc)_4$ — (orange), 12.85 g of sodium diethyldithiocarbamate (Sigma-Aldrich Corporation, St. Louis, MO) is dissolved in 200 mL of ethanol. Concurrently, 3.0 mL of tin tetrachloride (Sigma-Aldrich Corporation, St. Louis, MO) is dissolved in 50 mL of ethanol. The sodium diethyldithiocarbamate solution is added dropwise to the tin tetrachloride solution under constant stirring via a burette. Upon completion of the solution combination, the product is stirred for a further ten minutes, followed by ten minutes of ultrasonication, to ensure completion of the ion-replacement reaction. The product is then washed in ethanol and deionized water, separated via centrifuge, and washed again until the product is washed five times. The product is then dissolved in chloroform and dried under argon flow. The synthesized $Sn(dedc)_4$ is fully decomposed above 318 ºC (fig. 3.1.1).

To form copper diethyldithiocarbamate — $Cu(dedc)_2$ — (dark green/black), 9.0 g of sodium diethyldithiocarbamate (Sigma-Aldrich Corporation, St. Louis, MO) is dissolved in 150 mL of ethanol. Concurrently, 4.23 g of copper chloride (Sigma-Aldrich Corporation, St. Louis, MO) is dissolved in 50 mL of ethanol. The sodium diethyldithiocarbamate solution is added dropwise to the copper chloride solution under constant stirring via a burette. Upon completion of the solution combination, the product

is stirred for a further ten minutes, followed by ten minutes of ultrasonication, to ensure completion of the ion-replacement reaction. The product is then washed in ethanol and deionized water, separated via centrifuge, and washed again until the product is washed five times. The product is then dissolved in chloroform and dried under argon flow. The synthesized $Cu(dedc)_2$ is fully decomposed above 302 ºC (fig. 3.1.1).

3.2: Precursor Solution Chemsitry

The precursor solution used in the spray pyrolysis experiments outlined here is generally a combination of zinc, tin, and copper diethyldithiocarbamates dissolved in toluene. The amounts of the precursors must be calibrated with the apparatus in order to achieve the desired CZTS stoichiometry, as the system is not 100% efficient in converting the precursors into CZTS. This is hypothesized to be due to the complexity of crystalline CZTS, a quaternary kesterite-structured material, so the experimental conditions within the apparatus are difficult to set to the thermal conditions that are optimal to create CZTS (fig. 3.2.1).

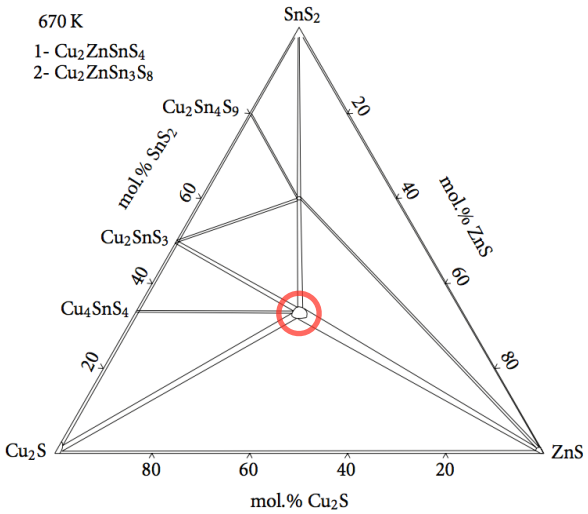

Figure 3.2.1: (From [2]) Effective ternary CZTS phase diagram from relative ratios of Cu_2S, SnS_2, and ZnS. Stoichiometric CZTS is circled in red.

Depending on the desired powder/thin film composition, the precursor solution is concocted by dissolving 361.9 mg $Zn(dedc)_2$ (white) in 60 mL toluene, then dissolving 711.8 mg $Sn(dedc)_4$ (orange) in the $Zn(dedc)_2$ + toluene solution, then dissolving 720.2 mg $Cu(dedc)_2$ (black) in the $Zn(dedc)_2$ + $Sn(dedc)_4$ + toluene solution. These amounts contain precisely a 2:1:1 Cu:Zn:Sn molar ratio (plus 20 parts sulfur, an excess of 16 moles per molecule), the ratio found in stoichiometric kesterite CZTS, though in practice, precursor conversion efficiency must be taken into account.

The $Cu(dedc)_2$ in particular is not fully soluble in toluene, but as long as the material is kept well-suspended in the precursor solution, it is uniformly distributed in the aerosol created by the nebulizer. To do this, the precursor solution is always allowed to ultrasonicate for at least 20 minutes before use, it is well-stirred before being added to the nebulizer jar, and it is kept under constant stirring while being nebulized.

The spray process, still, however, seems to be not totally efficient. The author has found that there are typically concentrated deposits of precursor left in the nebulizer after the completion of a run. This inefficiency eventually leads to non-

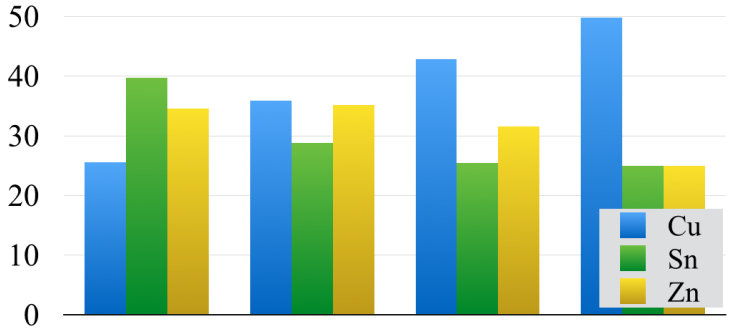

	$Cu(dedc)_2$	$Sn(dedc)_4$	$Zn(dedc)_2$
Sample 1	500 mg	500 mg	250 mg
Sample 2	500 mg	340 mg	180 mg
Sample 3	500 mg	180 mg	90 mg

Figure 3.2.2: Elemental atomic percentages of copper, zinc, and tin in three CZTS powder samples made with varying amounts of precursors.

stoichiometric CZTS production. To compensate, though, the composition of the powder can be controlled by varying the relative precursor ratios (fig. 3.2.2). By increasing the amount of $Cu(dedc)_2$ relative to $Zn(dedc)_2$ and $Sn(dedc)_4$, for example, as seen in the figure, the resulting powder stoichiometry increases in copper relative to zinc plus tin (determined by energy dispersive x-ray analysis — EDS — in scanning electron microscopy —SEM). The optimal precursor ratio in not exceedingly consistent, but has been found to be roughly five parts $Cu(dedc)_2$ to two parts $Sn(dedc)_4$ to one part $Zn(dedc)_2$.

Doping of CZTS material can also be achieved by including various additives to the precursor solution. In particular, sodium diethyldithiocarbamate and silicon nanoparticles (separately) have been added to the generic mixture to induce sodium and silicon doping into CZTS nanoparticles.

3.3: Synthesizing CZTS Thin Films/Platelets

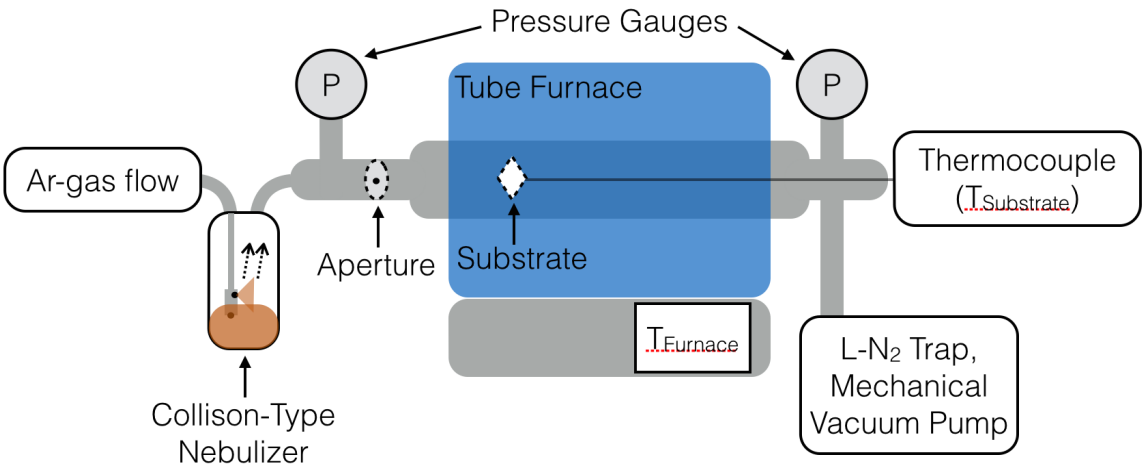

Figure 3.3.1: Aerosol spray pyrolysis system used to synthesize CZTS thin films.

To synthesize CZTS thin films, the spray pyrolysis apparatus is assembled as shown in fig. 3.3.1. The location of the substrate within the furnace allows for crystal nucleation and growth in one step, theoretically removing the need for an annealing step in a sulfur-rich atmosphere.

The precursor solution is aerosolized by the pressure differential caused by the flow of the carrier gas through the nebulizer head. In this apparatus, a one-jet nebulizer head is used, so the carrier gas (Ar) flow rate is limited to ~0.5 SCFH. The aerosol is then pulled through a focusing aperture (diameter of 1/8") and directed onto a substrate, fastened onto a stainless steel mount. The excess non-decomposed precursor, carrier gas, and decomposed diethyldithiocarbamate complexes are then pulled through the furnace by a rotary vane vacuum pump, and filtered by a liquid nitrogen trap, before proceeding to an exhaust tube.

The system is kept at an ambient pressure of ~225 torr during runs, measured on both sides of the furnace. Molybdenum-coated soda lime glass is the substrate of choice, as it makes an effective base for a PV cell. Blank quartz can also be used in order to obtain absorption measurements on the films. The furnace is set within a range of 350-500 ºC. Temperatures lower than this run the risk of not fully decomposing the precursors, while temperatures higher than this run the risk of damaging the molybdenum coating on the substrate. The location of the substrate within the furnace is variable. The system is typically run with the substrate a distance of ~45 cm away from the nebulizer

port. The substrate temperature is measured approximately by a thermocouple that is threaded through to touch the back side of the substrate mount. The substrate temperature is measured to be consistently 20 ºC below the ambient temperature of the furnace, which is attributed to the cooling effect of the aerosol and carrier gas colliding with the substrate.

The system is allowed to run until the nebulizer jar is empty, or as long as the user desires, depending on the desired thickness of the film. At the completion of a run, the carrier gas is stopped, the nebulizer is shut off from the furnace tube by a quarter-turn valve, and the furnace tube is pumped constantly until the furnace drops to a temperature below 300 ºC. The system is then opened, and the substrate is removed and the resulting film is characterized (see section 3.8).

3.4: Synthesizing CZTS Nanoparticles

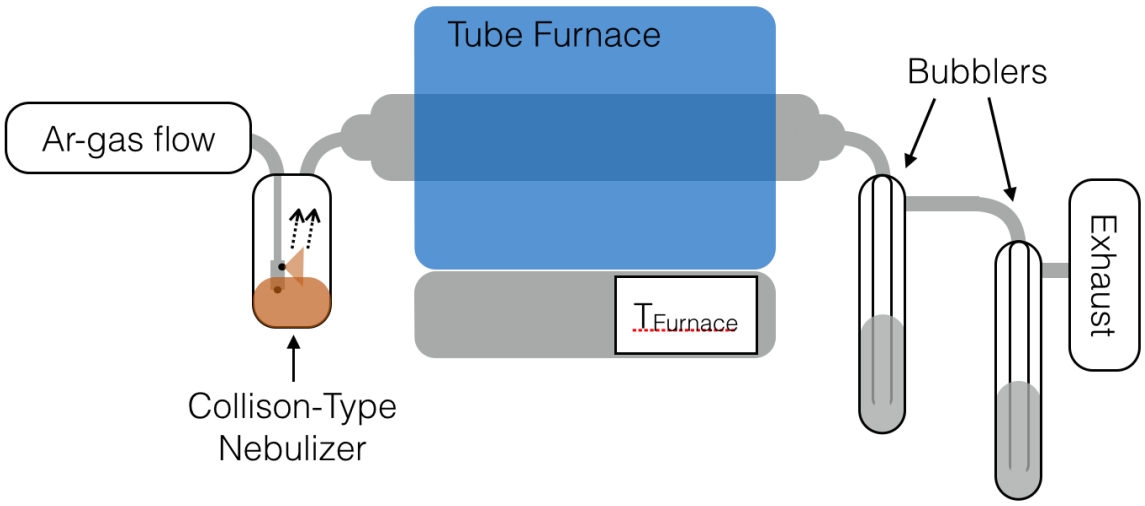

Figure 3.4.1: Aerosol spray pyrolysis system used to synthesize CZTS nanoparticles.

To synthesize CZTS nanoparticles, the spray pyrolysis apparatus is assembled as shown in fig. 3.4.1. The use of bubblers to collect the powder allows for operation at atmospheric pressure while keeping the system sealed from atmospheric gases.

The precursor solution is aerosolized by the pressure differential caused by the flow of the carrier gas through the nebulizer head. In this apparatus, a six-jet nebulizer head is used, the carrier gas (Ar) flow rate is set to ~12 SCFH for each run, which gives the aerosol droplets a residence time of 0.12 seconds in the thermal zone. The aerosol is then pushed into the tube furnace, where the thermal conditions are such that precursors decompose and form CZTS particles. The particles, along with the excess non-decomposed precursor, carrier gas, and decomposed diethyldithiocarbamate complexes are then pushed through two toluene-filled bubblers to separate the powder from gases. The solid material is left suspended in the bubblers.

At the end of a run, the material is washed five times with toluene and methanol to dissolve any diethyldithiocarbamate complexes or metal salts that may have formed and separated via centrifuge. The remaining particles are then dispersed in methanol and dried under argon flow. The material can then be characterized accordingly (see section 3.8).

During each run, the bubblers must be refilled with toluene as it evaporates in order to ensure good collection of solid material.

The optimal temperature at which to synthesize CZTS nanoparticles has been found to be 800 ºC (see results in section 4.2). At lower temperatures, the mass of

particles recovered diminishes significantly, while at higher temperatures, the particles are found to be embedded in an amorphous matrix.

3.5: Doping CZTS Nanoparticles

The elemental composition of CZTS thin films and nanoparticles can be tuned based on the relative precursor ratios (fig. 3.2.2), meaning that the apparatus provides a highly controllable method of forming CZTS structures. Further experiments have been performed studying the controllability of dopants in CZTS nanoparticles.

To dope the nanoparticles with sodium, sodium diethyldithiocarbamate — having the same molecular structure to the primary precursors — is added to the precursor solution.

The more difficult dopant is silicon. The desired effect is to replace some of the tin lattice sites with silicon. To add silicon to the CZTS nanoparticles, some of the tin precursor is subtracted from the precursor solution, while some silicon nanoparticles (diameter of ~10 nm, formed by a non-thermal plasma method [3], stored in an oxygen free environment) are added.

3.6: Coating CZTS Dispersions onto Substrates

To create thin films from CZTS nanoparticles, it is necessary to coat the particles uniformly on a substrate. In this work, CZTS are sprayed onto substrates using a Master® airbrush.

The dry CZTS nanoparticles are well-dispersed in methanol by ultrasonicating for >15 minutes. The solution is then added to the airbrush cup, and is turned into an aerosol, and sprayed onto a substrate. Compressed argon (99.97% pure) is used to generate the aerosol. To achieve a uniform coating, it is necessary to run the carrier gas at a low flow rate; here ~1 SCFH is used. The spray is directed onto a masked substrate in a uniform pattern until the desired thickness is achieved. It takes between 45 minutes and one hour to obtain a 1 µm-thick film. An exemplary coating is shown in fig. 3.6.1, both on the macro and micro scale.

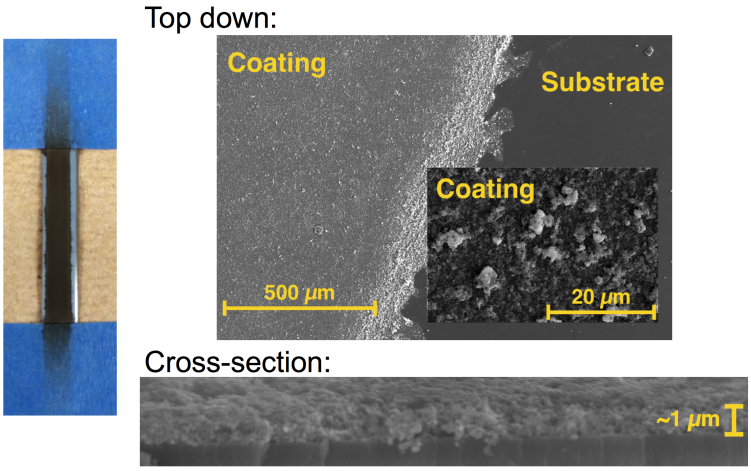

Figure 3.6.1: Macroscopic, SEM top down, and SEM cross section images of a coating of CZTS nanoparticles created using the process outlined in section 3.6.

Thus far, the coatings have been laid on a thermally oxidized silicon wafer, to allow easy characterization. In the future, the coatings will be applied to quartz, and molybdenum-coated soda lime glass for optical characterization and cell fabrication. The substrate is masked over a rectangular area using masking tape, which also serves to hold the substrate immobile and level. The substrate is also made twice as large as the desired film area, and is pre-scored. This is to allow easy splitting of the substrate and coating to give a control sample, as well as one that will be annealed.

3.7: Sintering CZTS Nanoparticles to form Crystalline Films

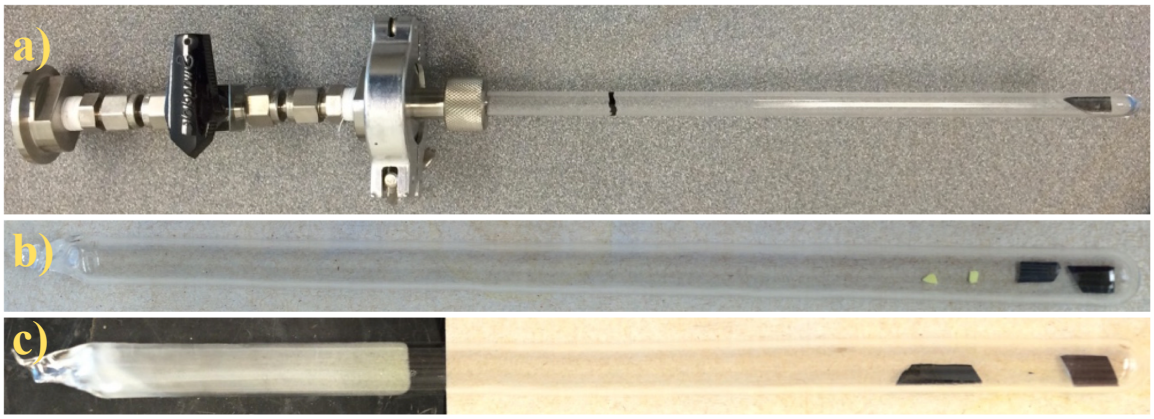

Figure 3.7.1: a) Shows an ampoule loaded with sample and elemental sulfur after pumping down to 10^{-5} torr. b) Shows an ampoule that has been sealed off to be eight inches long from image a. c) Shows an ampoule that has undergone the annealing procedure. Note the white deposit on the left side of the ampoule, that is the re-condensed sulfur. The light background on the right of image c has been added for contrast.

Once the CZTS nanoparticles have been coated onto a substrate, the sample must be baked in a sulfur-rich atmosphere to promote crystal grain formation and growth, as discussed in Section 2.7. To do this, the samples are sealed in an evacuated ampoule with some solid sulfur, and then placed inside a tube furnace for a designated duration.

The samples are placed in a 1/4" diameter quartz tube, with one end that has been closed off. Approximately 12 mg of sulfur are also added the tube, which when heated to 500 ºC — the boiling point of sulfur is 444.61 ºC [4] — will yield roughly atmospheric sulfur pressure (~700 torr) within the sealed and evacuated ampoule.

The quartz tube is then joined to an airtight apparatus via a Swagelok Ultra-Torr fitting to be pumped down to ~10^{-5} torr by a roughing rotary vane pump, and then a turbo-molecular pump (fig 3.7.1a). The ampoule is then closed off from the system by a

quarter-turn valve. The ampoule plus valve assembly is then removed from the apparatus and the ampoule is then sealed off so that it is eight inches long using an oxyacetylene torch.

The sealed ampoule is then inserted into a 500 ºC preheated 1-inch tube furnace and baked for 30 minutes. At the end of the bake, the ampoule is moved so that one end is slightly outside the furnace, while the end with the samples are still predominantly within the heating zone in the furnace. This allows the exposed end to cool more quickly, and thus the sulfur vapor condenses and solidifies away from the samples (fig 3.7.1c).

Upon cooling to below the boiling point of sulfur (444.7 ºC), the ampoule can be removed and allowed to cool uniformly in the ambient environment. Here, the ampoule is not removed from the furnace until it has cooled to below 300 ºC to give less probability of sulfur condensing on the samples. Once cooled, the ampoule is broken open and the samples are removed and characterized.

3.8: References

[1] Khare, Ankur, Andrew W. Wills, Lauren M. Ammerman, David J. Norris, and Eray S. Aydil. “Size Control and Quantum Confinement in Cu2ZnSnS4 Nanocrystals.” Chemical Communications 47, no. 42 (October 18, 2011): 11721–23. doi:10.1039/C1CC14687D.

[2] Schorr, S. Thin Solid Films, Proceedings of Symposium O, EMRS 2006 Conference EMRS 2006 Symposium O, 515, no. 15 (2007): 5985–91. doi:10.1016/j.tsf.2006.12.100.

[3] Mangolini, L., E. Thimsen, and U. Kortshagen. “High-Yield Plasma Synthesis of Luminescent Silicon Nanocrystals.” Nano Letters 5, no. 4 (April 1, 2005): 655–59. doi: 10.1021/nl050066y.

[4] *Tables of Physical & Chemical Constants*, Kaye & Laby Online, 16th edition, 1995. Version 1.0 (2005), accessed August, 2015.

Chapter 4: Results

4.1: Synthesis of CZTS Thin Films/Platelets

We have demonstrated that spray pyrolysis is not an effective method to synthesize CZTS thin films, and disseminated our results in [1]. Effectively, at low temperatures (~350-400ºC), the film does not deposit much at all, likely due to the incomplete decomposition of the precursors. At higher temperatures, the deposited material nucleates non-uniformly, particularly above ~440 ºC, at which point two-dimensional platelet structures nucleate above the substrate (fig. 4.1.1).

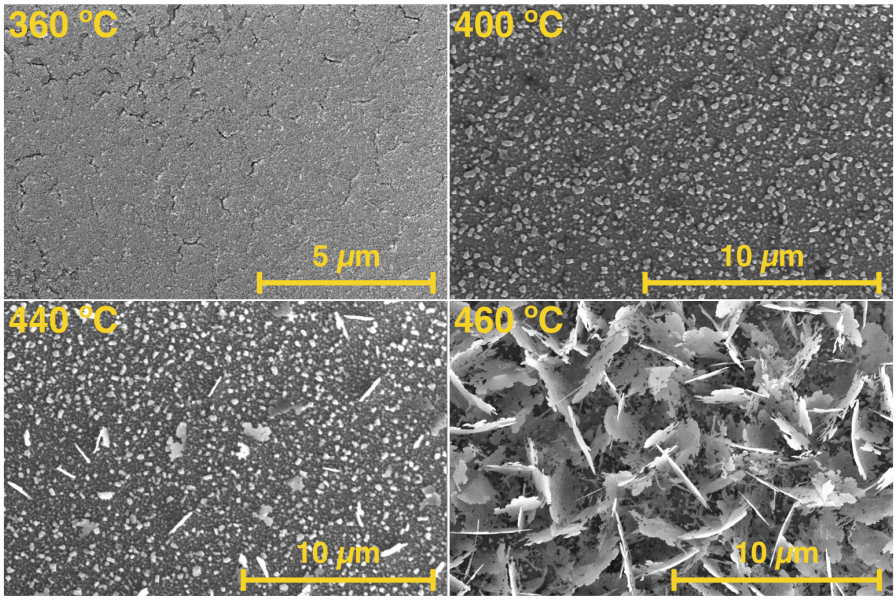

Figure 4.1.1: (From [1]) SEM micrographs of samples grown on molybdenum-coated soda lime glass at various temperatures.

The dominant variable associated with the structure and morphology of these films is temperature. Within a small temperature range (~350-500 ºC), there is an immense morphological development, ranging from a film of negligible thickness grown at 350 ºC, to a very complex morphological structure that is made up of two-dimensional

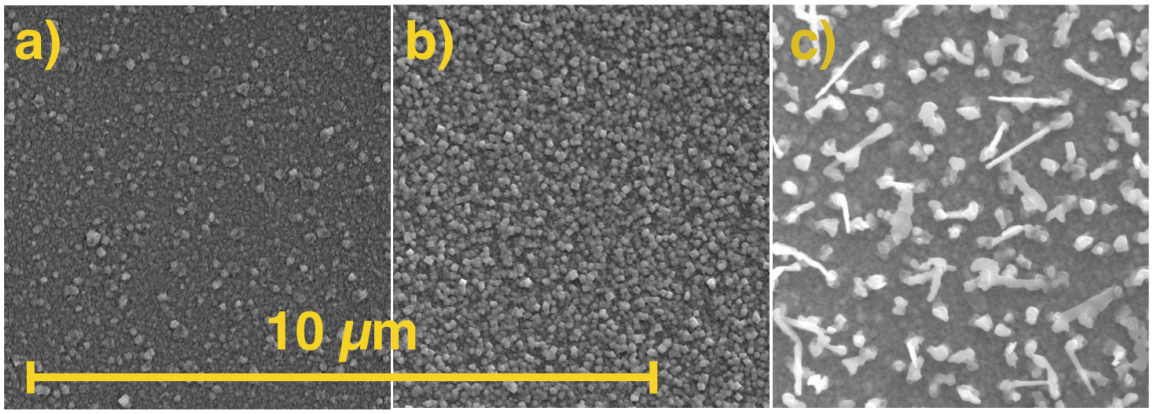

Figure 4.1.2: SEM micrographs of a) zinc sulfide, b) tin sulfide, and c) copper sulfide samples grown on molybdenum-coated soda lime glass each at 450 ºC.

platelet structures in a disorderly arrangement that increases the effective film thickness to 5-10 μm seen in films grown above 440 ºC.

This same apparatus and procedure has also been used to synthesize binary copper sulfide, tin sulfide, and zinc sulfide films. From these films, we attribute the platelet formation and nucleation to the presence of a copper sulfide phase. For tin sulfide and zinc sulfide films, nanostructured isotropic growth is observed. It is only in copper sulfide films where anisotropic growth is observed (fig. 4.1.2).

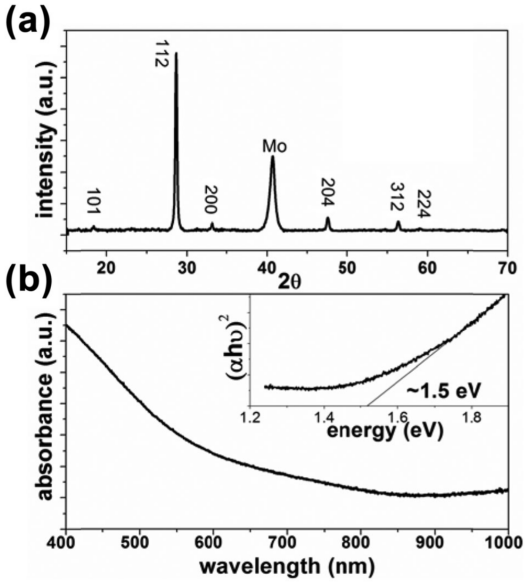

Figure 4.1.3: (From [1]) a) XRD of the sample grown at 460 ºC (see fig. 4.1.1). b) UV-vis absorbance for the sample grown at 460 ºC. The Tauc plot generated using the spectrum is shown in the inset.

Films synthesized at various temperatures within this growth range have been characterized extensively. XRD scans of

a sample with a prevalence of the two-dimensional platelet structures indicates the presence of kesterite-phase CZTS, while photospec. measurements allow the determination of the material's band gap, found to be ~1.5 eV (fig. 4.1.3). While the characteristic kesterite CZTS peaks in XRD match well with values reported in literature, the spectrum by itself is inconclusive proof, as it matches well with spectral peaks for other binary and ternary sulfides, like ZnS and Cu_2SnS_3 [2]. In combination with Raman, though, it is easier to be conclusive about the phase of the material.

Raman spectroscopy of samples grown across the 350-500 ºC temperature range shows an interesting development as temperature is increased. At the lower temperatures (360, 400 ºC), the Raman spectra show the presence of crystalline CZTS, but also molybdenum sulfide (MoS_2), suggesting that some of the precursors have decomposed, but the most thermodynamically favorable reaction is with the molybdenum substrate, instead of the other metal ions present. At the higher temperatures (440, 460 ºC), the Raman spectra show the

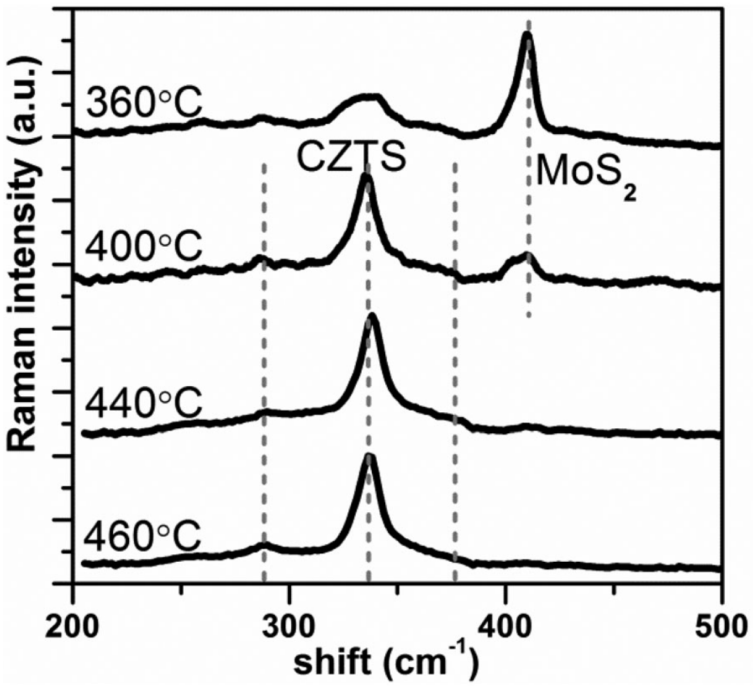

Figure 4.1.4: (From [1]) Thin film Raman spectra as a function of temperature.

T (ºC)	At. % Cu	At. % Zn	At. % Sn	At. % S	$\frac{[Cu]}{[Zn]+[Sn]}$	$\frac{[Zn]}{[Sn]}$
360	38.1(±1.6)	15.5(±0.6)	6.8(±0.5)	39.5(±2.0)	1.70	2.2
400	34.8(±0.8)	21.9(±0.5)	8.7(±0.3)	35.4(±1.6)	1.13	2.5
440	25.7(±0.8)	25.0(±0.7)	9.5(±0.5)	39.7(±1.9)	0.75	2.6
460	29.8(±1.0)	21.0(±0.6)	10.5(±0.4)	38.7(±1.6)	0.94	2.0

Table 4.1.1: (From [1]) Summary of the results from the elemental analysis performed by EDS on samples grown at different temperatures. The values correspond to atomic percentages and to their ratios.

disappearance of the MoS_2 peak, as well as narrower and more well defined — meaning more crystalline — CZTS peaks at 288, 338, and 380 cm^{-1} (fig. 4.1.4).

Elemental analysis of large areas on these films shows further support to the hypothesis that at the lower temperatures, the failure of film growth is due to the lack of precursor decomposition. Noting that the highest precursor decomposition temperature is 334 ºC for $Zn(dedc)_2$, at lower temperatures, there is an excess of copper — the precursor for which has the lowest decomposition temperature at 302 ºC. At higher temperatures,

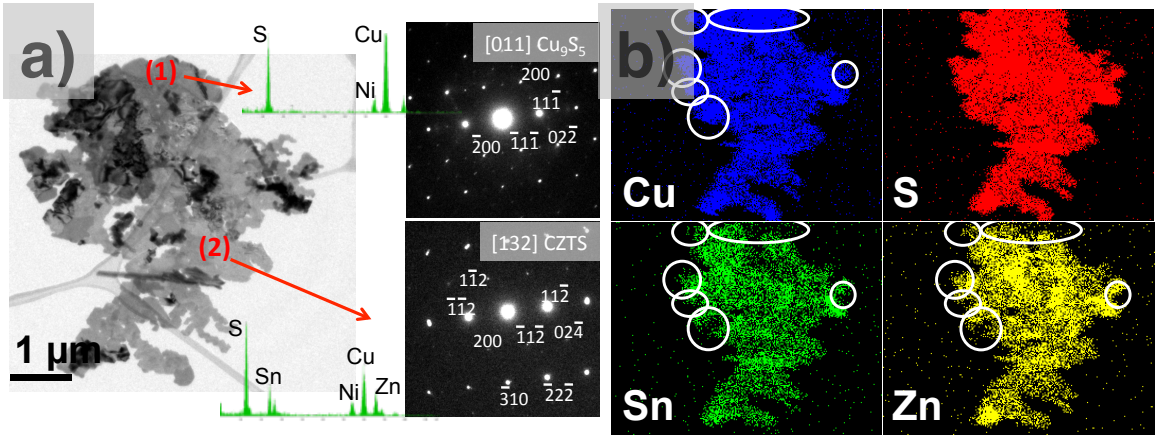

Figure 4.1.5: (From [1]) (a) TEM of a nanoplatelet grown at 460 ºC. EDS scans and selected area diffraction pattern for two spots are also shown. (b) Elemental mapping for the platelet in (a) showing the variation in the local composition.

the [Cu]/([Zn]+[Sn]) ratio levels out to ~1, which is ideal for stoichiometric CZTS (table 4.1.1). The elemental analysis was performed on areas ~100 μm square, meaning that any phase instability on individual platelets is inconsequential.

Elemental analysis has also been performed on individual platelets in TEM (fig. 4.1.5). The platelets are clearly crystalline, though the diffraction pattern suggests that multiple phases are present within a single platelet. Elemental mapping suggests that the bulk of the platelets could be kesterite CZTS, while the phase impurity is focused on the edges, where an excess of copper relative to zinc and tin is seen.

It is hypothesized that the copper sulfide has a chance to nucleate as a binary sulfide because the corresponding precursor has the lowest decomposition temperature. Once the copper sulfide has nucleated, it is thermodynamically stable, and will not change phase, though it appears to catalyze the formation of anisotropic platelet growth and the formation of kesterite CZTS.

While interesting, these findings suggest that spray pyrolysis is an ineffective method for synthesizing CZTS thin films for PV applications. In order to make an effective PV, it is necessary for the interface between each layer to have exceptional contact, so that little charge is lost between the different materials. Since the inherent problem with the application of the CZTS material system to PVs lies in charge loss and defects within the material, an alternative method of CZTS synthesis — nanoparticle formation and sintering — has been explored.

4.2: Synthesis of CZTS Nanoparticles

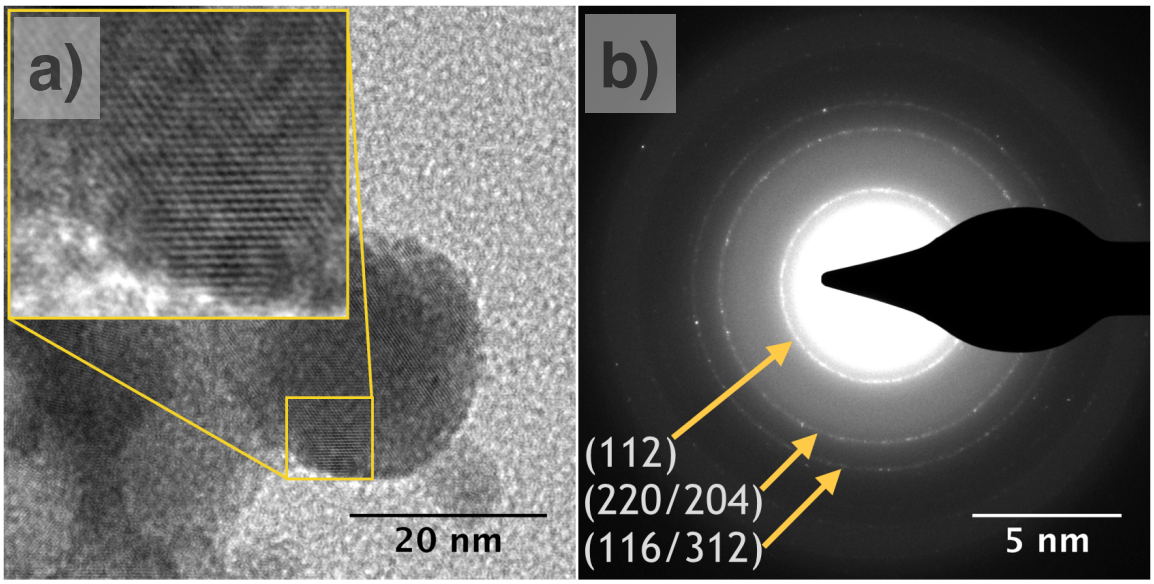

Figure 4.2.1: (a) TEM of a nanoparticle grown at 800 ºC. Inset provided to better observe uniform crystal fringes. (b) Diffraction pattern of particle shown in (a), three primary fringes align well with primary kesterite-CZTS peaks.

Using aerosol spray pyrolysis to synthesize CZTS nanoparticles appears to be more advantageous than using the process to synthesize CZTS films, mainly due to its economic and scalable application to the technology's marketability. The process can be separated into a few distinct steps to go from

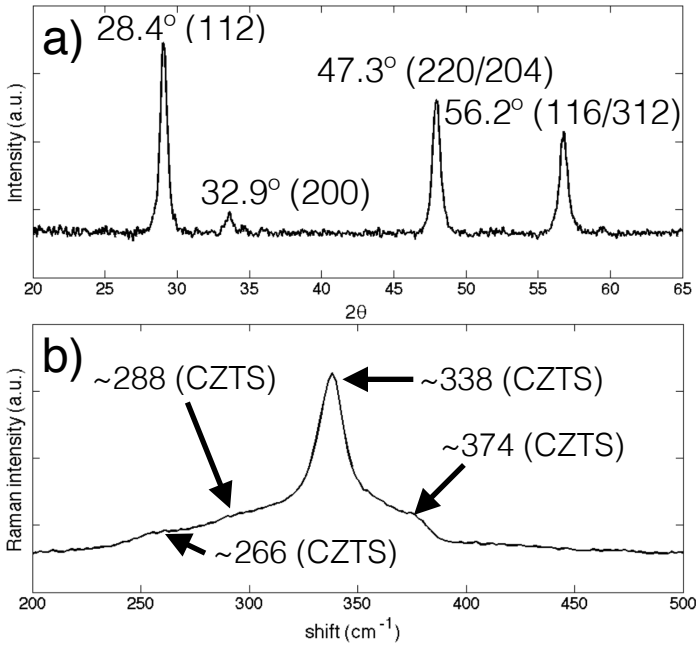

Figure 4.2.2: (a) Shows an XRD spectrum of nanoparticles grown at 800 ºC and (b) Raman spectrum of same nanoparticles.

precursor material through to uniform, crystalline CZTS thin films. Discussed here are results found when attempting to synthesize and control the composition of CZTS nanoparticles.

We have shown the ability to consistently create crystalline kesterite-CZTS nanoparticles with a narrow size distribution centered around ~20 nm in diameter (fig. 4.2.1). Further characterization of these particles via XRD and Raman confirms the presence of kesterite-phase CZTS (fig. 4.2.2).

With the ability to create nanocrystalline CZTS confirmed, the controllability of the system needed to be assessed. To do this, the system was run with one parameter variable at a time. A study of the effect of running at different furnace temperatures and of using altered precursor ratios in the precursor solution (i.e. the amount of $Cu(dedc)_2$ relative to $Zn(dedc)_2$ and $Sn(dedc)_4$).

By running the system at temperatures from as low as 400 ºC to as high as 1,000 ºC, it was determined that the optimal running temperature is approximately 800 ºC, and so has been settled on as the standard operating temperature for the system.

Below this optimal temperature, there is a marked decline in the amount of powder produced and collected, implying that the precursor doesn't fully decompose fully at lower temperatures. While the furnace is set above the decomposition temperature for all three precursors even at 400 ºC, the residence time of the aerosol droplets within the furnace is too short (~0.12 s) to allow an adequate amount of thermal energy to be radiated into the droplets to cause decomposition of the precursors, hence the high

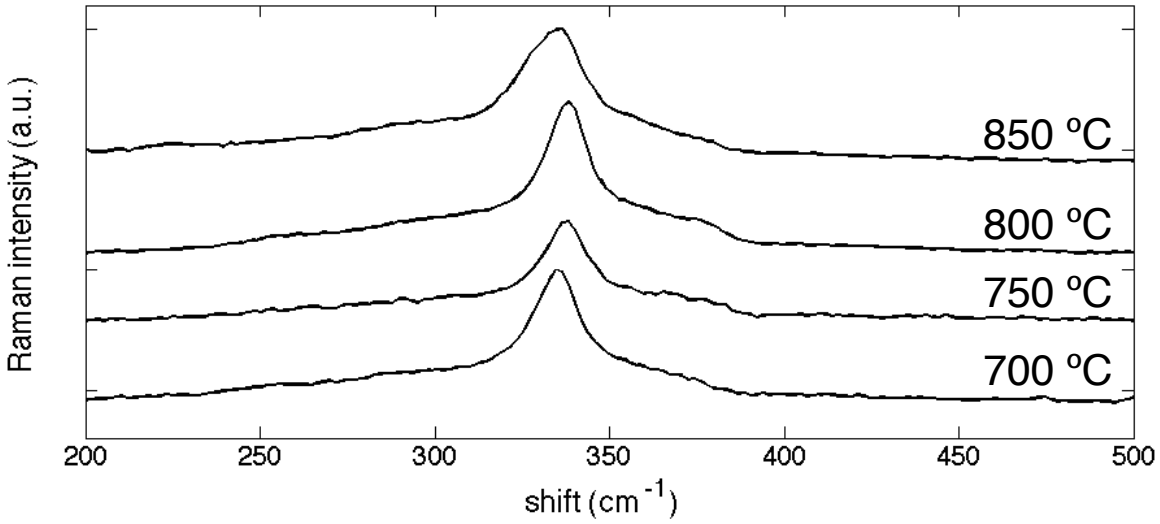

Figure 4.2.3: Shows Raman spectra of CZTS nanopowders grown at various temperatures.

temperature is necessary. The crystalline powder collected is still indicated to be kesterite-CZTS by Raman (fig. 4.2.3).

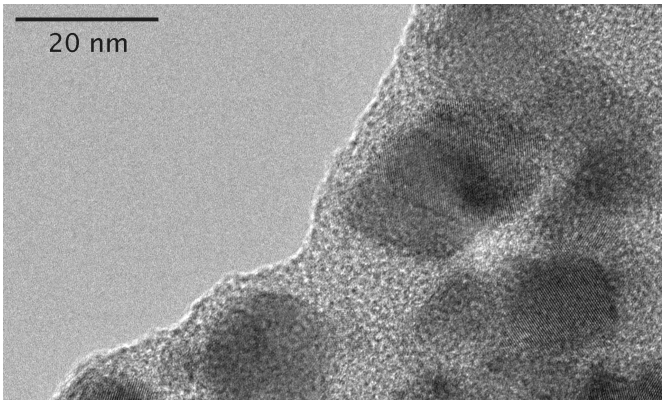

Figure 4.2.4: TEM micrograph of sample grown at 900 ºC showing crystalline CZTS powder embedded in amorphous matrix.

Above the optimal 800 ºC temperature, the powder is still formed as crystalline CZTS, but TEM indicated the powder is embedded in an amorphous matrix (fig. 4.2.4). Cursory analysis via Fourier Transform Infrared Spectroscopy indicates that the amorphous material is likely organic in composition, making it undesirable for the material system.

Then, by running the spray pyrolysis system with variable relative precursor ratios, the controllability of the material composition has been examined. The material

	$Cu(dedc)_2$	$Sn(dedc)_4$	$Zn(dedc)_2$	At. % Cu	At. % Zn	At. % Sn	$\frac{[Cu]}{[Zn]+[Sn]}$
S1	500 mg	500 mg	250 mg	25.59	34.62	39.79	0.34
S2	500 mg	340 mg	180 mg	35.96	35.16	28.88	0.56
S3	500 mg	180 mg	90 mg	42.87	31.60	35.53	0.63

Table 4.2.1: Summary of the results from the EDS performed on samples grown from different precursor ratios.

stoichiometry has been shown to be highly controllable, though it is clear that the system is incapable of perfectly converting all of the precursor into CZTS effectively, as observed in Table 4.2.1 — a summary of EDS analysis performed on powder formed with varied precursor concentrations.

Perfect precursor conversion would achieve the ideal relative copper : zinc : tin ratio with a relative $Cu(dedc)_2$: $Zn(dedc)_2$: $Sn(dedc)_4$ mass ratio of approximately 2:2:1 (used in Sample 1 of table 4.2.1). However, ideal CZTS stoichiometry was approached as both tin and zinc precursors were decreased relative to copper precursor, implying the copper precursor is more difficult to convert than the others. This is likely due to the fact that $Cu(dedc)_2$ has been observed to be imperfectly soluble in toluene, so there is a depletion of this precursor in the aerosol droplets unless it's concentration is increased.

This data provides evidence that the aerosol spray pyrolysis system described here is capable of controllably producing phase-pure kesterite-CZTS.

4.3: Doping of CZTS Nanoparticles

Sodium is a common dopant in the CIGS and CZTS systems [3, 4]. In CZTS, Johnson *et al* showed that crystal grain size increased when annealing films of cosputtered copper, zinc and tin on a soda lime glass (SLG) substrate in a sulfur rich atmosphere as opposed to a quartz or pyrex glass substrate [4]. The conclusion made is that impurities in the SLG — particularly alkali metals — diffuse into the CZTS film and drive crystal grain growth, which is a potential factor in PV conversion efficiency.

It stands to reason that the presence of these alkali metals, namely sodium, in CZTS nanoparticles will drive the growth of large crystal grains during annealing. Results suggesting as much have been shown by Chernomordik *et al* in [5].

The method of doping sodium into CZTS in [4] and [5] relied on diffusion from external sources, namely SLG substrates or coatings of alkali hydroxides on ampoule surfaces. The ability to more controllably dope sodium into the system without relying on a particular substrate would allow the crystal grain growth effect to be better studied and understood.

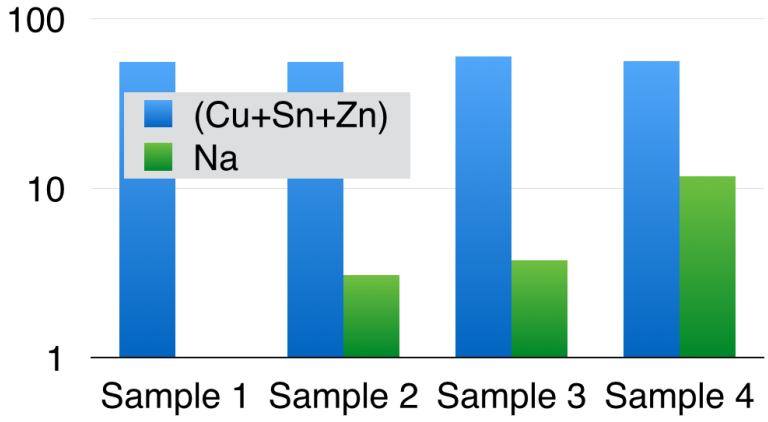

Figure 4.3.1: Chart showing amount of sodium relative to copper, zinc and tin in powder grown with varying amounts of Na(dedc) mixed in with precursor solution characterized by EDS. Sample 1: 0 mg; Sample 2: 25 mg; Sample 3: 50 mg; Sample 4: 250 mg. Note the vertical scale is logarithmic.

Preliminary data

shows the ability to controllably dope sodium into CZTS nanoparticles via aerosol spray pyrolysis. The experimental parameters, described in section 3.5 are simple. Samples were grown at 800 ºC using 500 mg $Cu(dedc)_2$, 180 mg $Sn(dedc)_4$, 90 mg $Zn(dedc)_2$, plus 0, 25, 50, or 250 mg Na(dedc). The resulting powder was then characterized by EDS, and the results are shown in Fig. 4.3.1. Further analysis is required to determine whether the sodium is truly incorporated into the CZTS lattice, and whether or not the result is repeatable, but the data already collected suggests that the amount of sodium incorporated into the powder is simply dependent on the amount of sodium precursor in the precursor solution, as might be expected.

Doping silicon into CZTS is a much more experimental idea. In 1987, Chen *et* al at Boeing added gallium as a dopant to the copper-indium-selenide system [6]. The dopant gallium increased the photo-conversion efficiency of the material up to 10.1% a marked improvement on previous iterations, and spawned the CIGS system, which has been further improved and commercialized since.

This lattice-replacement doping mechanism — replacing a large Group III atom with a smaller atom from the same column in the periodic table — could also potentially be viable in the CZTS system. We propose replacing some of the tin in the kesterite-CZTS with the much smaller silicon — both being group IV elements.

The mechanism for introducing silicon via the same spray pyrolysis apparatus is outlined in section 3.5. The challenge would be to reach a thermal region where the silicon nanoparticles can be dissociated and incorporated into the CZTS matrix.

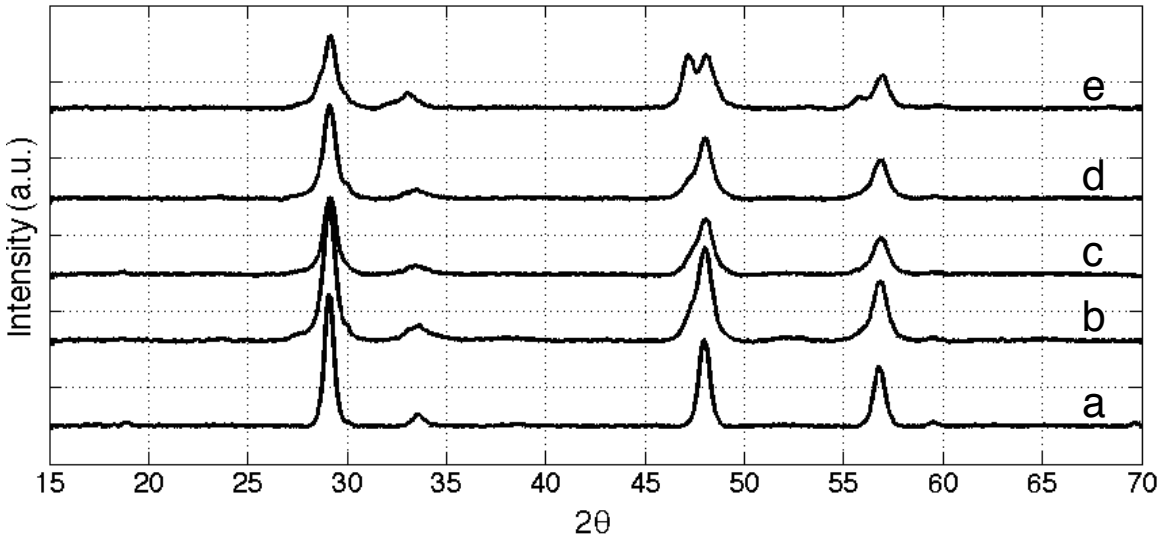

Figure 4.3.2: XRD spectra of five different samples showing the capability to incorporate silicon into CZTS nanoparticles. a) Made with 0 mg Si nanoparticles, 125 mg $Sn(dedc)_4$, b) made with 10 mg Si nanoparticles and 100 mg $Sn(dedc)_4$, c) made with 15 mg Si nanoparticles and 75 mg $Sn(dedc)_4$, d) made with 20 mg Si nanoparticles and 50 mg $Sn(dedc)_4$, and e) made with 20 mg Si nanoparticles and 0 mg $Sn(dedc)_4$.

Preliminary XRD characterization of particles grown with decreasing amounts of tin precursor and increasing amounts of silicon nanoparticles is shown in Fig. 4.3.2. An attempt was made to account for the inefficiency of the precursor-to-powder conversion of the apparatus, so more silicon and tin precursor were added than necessary to achieve the attempted silicon and tin combined concentrations in the final powder. It is apparent that the CZTS spectrum, seen in 4.3.2a, is affected by subtracting tin and adding silicon, though it is difficult to determine whether or not the silicon is truly incorporated into the kesterite lattice without further characterization of this powder — primarily Raman and TEM. The spectrum seen in 4.3.2e could just be a combination of the kesterite and silicon characteristic spectra.

In short, the aerosol spray pyrolysis in discussion here shows the potential to be able to controllably introduce a variety of dopants to CZTS nanoparticles.

4.4: CZTS Nanoparticle Annealing

Preliminary efforts have been made to sinter CZTS nanoparticles into uniform, large-crystal-grained films. Using the process outlined in section 3.7, several attempts have been made to coat and anneal CZTS nanoparticles made via the spray pyrolysis system.

The coatings (fig. 3.6.1) come out uniformly and consistently, though the thickness is hard to control as the coating duration is somewhat arbitrary, and the efficiency of coating the powder via the airbrush is unknown.

The results to this point haven't been exceedingly positive. In general, the films are annealed for 30 minutes at 500 ºC with 0.5-1 atm of sulfur pressure inside the ampoule (similar to

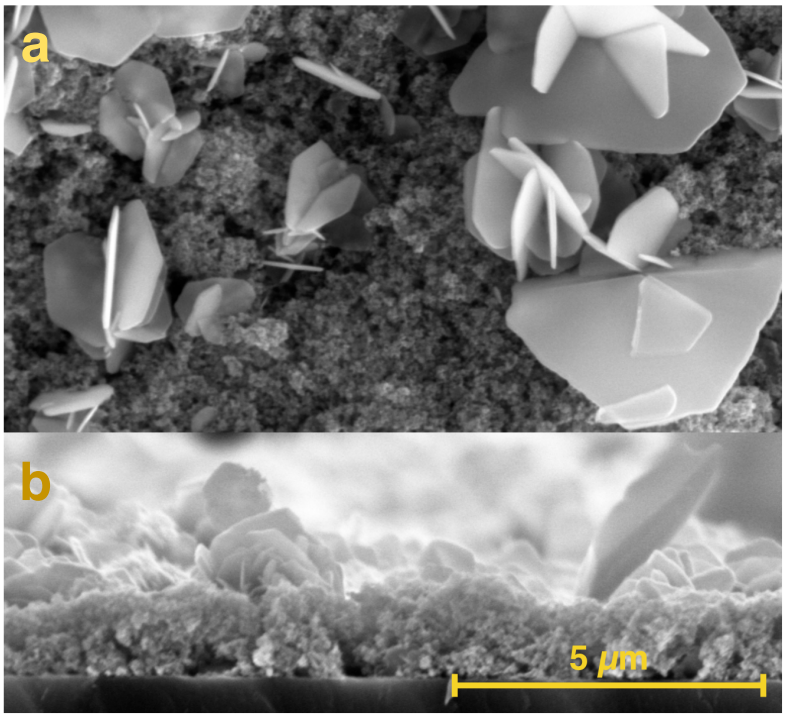

Figure 4.4.1: Shows top down (a) and cross section (b) SEM images of annealed CZTS sample with segregated structures observed on the surface of the film.

[7]). However, there are large two-dimensional structures that diffuse out of the film and form on the surface of the film, as seen in Fig. 4.4.1.

By EDS elemental mapping, it is apparent that these segregated structures must be some form of tin sulfide (fig. 4.4.2). The presence of tin is concentrated in the areas where the structures are present (fig. 4.4.2 spots 1 and 2 in d) and e)), while at the same time there is a deficiency of copper and zinc in those same areas (fig. 4.4.2 spots 1 and 2 in b) and c)).

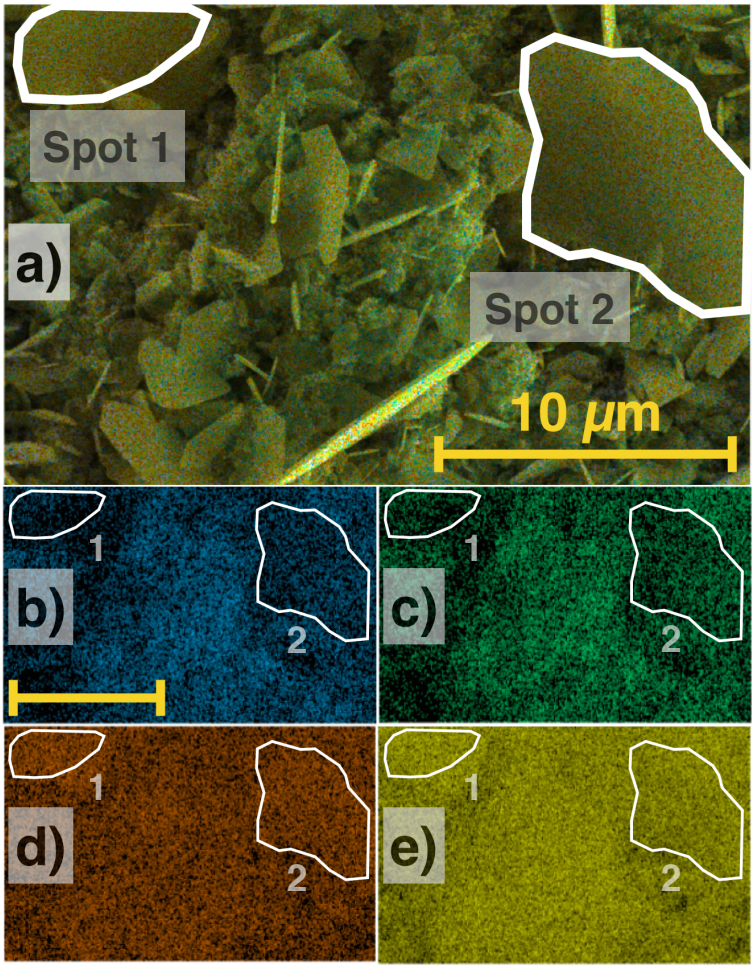

Figure 4.4.2: Shows EDS elemental mapping of the one spot on an annealed CZTS sample. a) Shows all maps combined together. b) Shows presence of copper L-α signatures. c) Shows presence of zinc L-α signatures. d) shows presence of tin L-α signatures. e) shows presence of sulfur K-α signatures. Spots 1 and 2 demarcate regions where large plate structures are visible. Scale bar for b)-d) is uniform at 10 μm.

More work needs to be done to determine the optimal conditions to form a uniform, large-grained CZTS film from a coating of CZTS nanoparticles. This is an integral step in fabricating thin film PVs, and current research in the field indicates that

decreasing the defect and impurity concentrations in the p-type layer is crucial to achieving high photo-conversion efficiency (see section 2.3).

4.5: References

[1] Exarhos, S., K. N. Bozhilov, and L. Mangolini. “Spray Pyrolysis of CZTS Nanoplatelets.” Chemical Communications 50, no. 77 (August 28, 2014): 11366–69. doi: 10.1039/C4CC05162A.

[2] Cheng, A.-J., M. Manno, A. Khare, C. Leighton, S. A. Campbell, and E. S. Aydil. “Imaging and Phase Identification of Cu2ZnSnS4 Thin Films Using Confocal Raman Spectroscopy.” Journal of Vacuum Science & Technology A 29, no. 5 (September 1, 2011): 051203. doi:10.1116/1.3625249.

[3] Niki, Shigeru, Miguel Contreras, Ingrid Repins, Michael Powalla, Katsumi Kushiya, Shogo Ishizuka, and Koji Matsubara. “CIGS Absorbers and Processes.” Progress in Photovoltaics: Research and Applications 18, no. 6 (September 1, 2010): 453–66. doi: 10.1002/pip.969.

[4] Johnson, M., S. V. Baryshev, E. Thimsen, M. Manno, X. Zhang, I. V. Veryovkin, C. Leighton, and E. S. Aydil. “Alkali-Metal-Enhanced Grain Growth in Cu2ZnSnS4 Thin Films.” Energy & Environmental Science 7, no. 6 (May 22, 2014): 1931–38. doi: 10.1039/C3EE44130J.

[5] Chernomordik, Boris D., Amélie E. Béland, Donna D. Deng, Lorraine F. Francis, and Eray S. Aydil. “Microstructure Evolution and Crystal Growth in Cu2ZnSnS4 Thin Films Formed By Annealing Colloidal Nanocrystal Coatings.” Chemistry of Materials 26, no. 10 (May 27, 2014): 3191–3201. doi:10.1021/cm500791a.

[6] Chen, W. S., J. M. Stewart, B. J. Stanbery, W. E. Devaney, and R. A. Mickelsen. “Development of Thin Film Polycrystalline CuIn1-xGaxSe2 Solar Cells,” 1445–47, 1987. http://adsabs.harvard.edu/abs/1987pvsp.conf.1445C.

[7] Chernomordik, B. D., A. E. Béland, N. D. Trejo, A. A. Gunawan, D. D. Deng, K. A. Mkhoyan, and E. S. Aydil. “Rapid Facile Synthesis of Cu2ZnSnS4 Nanocrystals.” Journal of Materials Chemistry A 2, no. 27 (June 17, 2014): 10389–95. doi:10.1039/C4TA01658K.

Chapter 5: Conclusions/Recommendations

5.1: Conclusions

Solar energy, along with other renewable source-based energy, is projected to play a large part in our domestic power generation within the next half-century. The effort to decrease PV system cost comes in part from decreasing the processing and material costs of fabricating a PV module itself, from reducing other costs associated with tying the power generation to the electricity grid, and also from human costs, like installing, permitting, and inspecting PV systems. In the roughly sixty years that PVs have been sold commercially, these costs have already been dramatically slashed via important technological innovations to PV module fabrication. Thick single crystal silicon-based PVs have given way to thin film PVs, which in the future will give way to sustainable material-based thin film PVs, such as CZTS. By working to further increase the affordability of small-scale residential PV systems as well as large-scale industrial PV systems, the growth of the sector will be stimulated at the expense of non-renewable energy sources like coal, oil, or natural gas.

Currently, CZTS as a thin film PV absorber layer is not technologically ready to be introduced in a commercial market, as the photo-conversion efficiency of even the best lab-scale devices is incomparable to other technologies, like crystalline silicon, CIGS, or CdTe. Recent efforts have also focused on synthesizing CZTS absorber layers in a more inexpensive and industrially scalable manner. Recent work has been done synthesizing both thin films and nanoparticles, which can be sintered into thin solid films.

One such method of synthesizing CZTS thin films and nanoparticles — presented here — is via spray pyrolysis.

While spray pyrolysis has been previously studied as a method of synthesizing CZTS thin films using single-source diethyldithiocarbamate precursors by other groups, it has not been shown conclusively to be an effective method of doing so. We similarly conclude that the crystallinity of said films is poor, and the film material is not phase-pure. Further, we hypothesize that the separation of platelet structures above the surface of the sprayed thin films suggests a copper sulfide phase impurity acts as a catalyst for non-uniform morphological development.

Our work suggests that spray pyrolysis synthesis of CZTS nanoparticles using single-source diethyldithiocarbamate precursors is a more viable method of forming CZTS by this process. We find the composition and crystallinity to be consistent with kesterite CZTS formed by other methods. Further, we show the composition to be tunable simply by adjusting the relative precursor ratios in the precursor solution. The process also shows promise in being able to controllably dope the powder with sodium or silicon by adding material to the precursor solution. Our current efforts are focused on determining the optimal conditions by which to sinter these nanoparticles into large-crystal grain thin films, which can then be used as the absorber layer in a PV cell, the ultimate goal of this project.

5.2: Future Work

Short term progression of this work will focus on material innovation and optimization, particularly involved with the doping of CZTS, preliminary results for which are outlined in Section 4.3. The benefits of incorporating either sodium or silicon as replacement or interstitial defects in the kesterite CZTS lattice are as yet unclear. The ability to controllably achieve uniform material doping with these materials, however, allow the opportunity to understand any effects, positive or negative, on photovoltaic performance.

In the long term, this project will continue in developing infrastructure to be able to fabricate working PV devices based on the CZTS material made by the process outlined here. The integral steps for this progression include optimizing the nanoparticle sintering process outlined in Section 4.4. This includes determining the appropriate nanoparticle stoichiometry, sulfur vapor pressure, sintering temperature, and sintering duration to achieve a uniform, large-crystal grain, stoichiometrically accurate thin film. Beyond this will come the optimization of the heterojunction partner to the photo-absorber layer — a thin n-type layer. Eventually a full photovoltaic cell can be constructed based on this absorber-emitter heterojunction structure.